

SUBGRADE STABILIZATION USING ALKALI ACTIVATED RICE HUSK ASH

PROJECT REPORT

Submitted by

MOHAMMED ZAYAN

Reg. No.: TKM21CETE10

to

the A P J Abdul Kalam Technological University

in partial fulfillment of the requirements for the award of the Degree

of

Master of Technology in

Transportation Engineering



Department of Civil Engineering

TKM College of Engineering, Kollam

May 2023

DECLARATION

I undersigned hereby declare that the project report "Subgrade Stabilization Using Alkali Activated Rice Husk Ash", submitted for partial fulfillment of the requirements for the award of degree of Master of Technology of the APJ Abdul Kalam Technological University, Kerala is a bonafide work done by me under supervision of Prof. Anandu V G. This submission represents my idea in my own words and where ideas or words of others have been included, I have adequately and accurately cited and referenced the original sources. I also declare that I have adhered to ethics of academic honesty and integrity and have not misrepresented or fabricated any data or idea or fact or source in my submission. I understand that any violation of the above will be a cause for disciplinary action by the institute and/or the University and can also evoke penal action from the sources which have thus not been properly cited or from whom proper permission has not been obtained. This report has not been previously formed the basis for the award of any degree, diploma or similar title of any other University.

Kollam

Mohammed Zayan

10/05/2023

DEPARTMENT OF CIVIL ENGINEERING

TKM College of Engineering, Kollam



CERTIFICATE

Certified that this report entitled '**SUBGRADE STABILIZATION USING ALKALI ACTIVATED RICE HUSK ASH**' is the report of the project presented by **MOHAMMED ZAYAN, Reg. No. TKM21CETE10**, during the year 2022-2023 in partial fulfillment of the requirement for the award of Degree of Master of Technology in Transportation Engineering of the APJ Abdul Kalam Technological University.

Guide

Prof. Anandu V G
Assistant Professor,
Dept. of Civil Engg.
TKMCE, Kollam

Coordinator

Dr. Adarsh S
Professor ,
Dept. of Civil Engg
TKMCE, Kollam

Head of the Department

Dr. Sajeed R.
Professor,
Dept. of Civil Engg.
TKMCE, Kollam

ACKNOWLEDGEMENT

I take this opportunity to express my deep sense of gratitude and sincere thanks to all who helped me to complete this project successfully.

I am deeply indebted to my guide, **Prof. Anandu V G**, Assistant Professor, Department of Civil Engineering for his excellent guidance, positive criticism and valuable assistance for the preparation of this project.

I am greatly thankful to the project coordinator, **Dr. Adarsh S**, Professor, Department of Civil Engineering for his constant supervising as well as for providing necessary information regarding the project.

I am greatly thankful to **Dr. Sajeeb R.**, Professor and Head of the Department of Civil Engineering.

I would also like to convey my sincere thanks to my parents and friends, without whose help this thesis would not have been a success.

Above all, I thank the almighty God for the successful conduct of this thesis.

MOHAMMED ZAYAN

ABSTRACT

The pavement performance is determined by the behaviour of the subgrade soil and its bearing capacity. Expansive subgrade soil is problematic to the pavement and other types of construction activities due to its excessive swelling and shrinkage, necessitating stability with various materials. Soil stabilization using different chemicals have been used to improve the soil property to make them suitable for the desired engineering purpose. Expansive subgrade can be stabilized using alkali activated slag, fly ash and other waste materials and this also helps in solving disposal difficulties. The purpose of the current work is to strengthen Black Cotton Soil (BCS) with alkali activated Rice Husk Ash (RHA) and to design flexible pavement using IITPAVE software (based on IRC 37-2018). This research explains the behaviour of the modified expansive soil for highway subgrade with liquid alkaline activator stabilizer and RHA. A combination of sodium hydroxide and sodium silicate was utilized as the liquid alkaline activators. Sodium oxide (Na_2O) and silica modulus (M_s) are the activator parameters selected for the investigation and were varied in different proportions. Unconfined Compression Strength test and Durability test were used to study the effect of different proportions of alkali activated RHA and activator parameters at different curing durations. CBR test, Swelling test and Flexural strength test were done on samples that have passed the Durability test and Unconfined Compressive Strength (UCS) with the highest compressive strength. This soil treatment enhanced the CBR, UCS, durability and flexural strength of the BCS. The swelling was also significantly reduced.

Keywords: *Soil stabilization, alkali activation, rice husk ash, sodium oxide, silica modulus*

TABLE OF CONTENTS

ACKNOWLEDGEMENT	i
ABSTRACT	ii
TABLE OF CONTENTS	iii-v
LIST OF FIGURES	vi-vii
LIST OF TABLES	viii
1. INTRODUCTION	1
1.1. General	1
1.2. Relevance of the Study	2
1.3. Objective of the Study	2
1.4. Organization of the Report	3
2. LITERATURE REVIEW	4
2.1. General	4
2.2. Alkali Activation Mechanism	4
2.3. Combination of Precursors	6
2.3.1. Volcanic Ash and Slag	6
2.3.2. Fly Ash and Slag	6
2.3.3. Slag and Paper Sludge Ash	7
2.3.4. Calcium Carbide Residue and Fly Ash.	7
2.3.5. Slag, Fly Ash and Ordinary Portland Cement	8
2.3.6. Slag and Fly Ash (added with construction and Demolition waste)	8
2.4. Addition of Fibers	9

2.4.1. Fly Ash, Slag and Polypropylene Fibers/Glass Fibers	9
2.4.2. Fly Ash and Coir Fibers	9
2.4.3. Fly Ash, Slag and Coir Fibers/Hemp Fibers	9
2.5. Slag as Precursor	9
2.6. Fly Ash as Precursor	12
2.7. Analysis of Pavement in IITPAVE	13
2.8. Closure	13
3. METHODOLOGY	14
3.1. General	14
3.2. Detailed Methodology	14
3.3. Sample Collection and Preliminary Tests	15
3.4. Specimen Preparation	15
3.5. Laboratory Tests	17
3.5.1. Liquid Limit Test	18
3.5.2. Plastic Limit Test	18
3.5.3. Proctor Compaction Test	19
3.5.4. CBR Test	19
3.5.5. Hydrometer Analysis	19
3.5.6. Unconfined Compression Strength Test	20
3.5.7. Swelling Test	20
3.5.8. Durability test	22
3.5.9. Flexural Strength Test	22
3.6. Pavement Design in IITPAVE	23
3.7. Closure	24
4. RESULTS AND ANALYSIS	25
4.1. General	25

4.2. Preliminary Tests	25
4.2.1. Atterberg Limits	25
4.2.2. Sieve Size Analysis	26
4.2.3. Proctor Compaction Test	27
4.2.4. CBR Test	28
4.2.5. Unconfined Compression Strength Test	28
4.3. Laboratory Test on Stabilized Soil Samples	29
4.3.1. Unconfined Compression Strength Test	29
4.3.2. Durability Test	37
4.3.3. CBR Test	38
4.3.4. Swelling Test	40
4.3.5. Flexural Strength Test	40
4.4. Pavement Design	41
4.5. Closure	
5. SUMMARY AND CONCLUSION	45
5.1. Summary	45
5.2. Conclusions	45
5.3. Research Contributions	46
5.4. Limitations and Future Scope	46
REFERENCES	47
APPENDIX	51

LIST OF FIGURES

Figure 2.1	Flow chart of Alkali Activation	5
Figure 2.2	Formed Geopolymer Network	6
Figure 2.3	Hydraulic Conductivity Results	8
Figure 2.4	Shear Strength Parameter Variation	8
Figure 2.5	Variation in Mass Loss	11
Figure 2.6	Variation in UCS	11
Figure 2.7	Variation in Free Swell Ratio	12
Figure 3.1	Methodology Flow Chart	14
Figure 3.2	Sample Combinations	16
Figure 3.3	RHA Used for the Study	17
Figure 3.4	Chemicals Used for the Study	17
Figure 3.5	Soil Used for the Study	18
Figure 3.6	Preparation of CBR Specimens	19
Figure 3.7	Casted Specimens for Compression Test	20
Figure 3.8	Swelling Test on Soil	21
Figure 3.9	Soil Immersed in Water	22
Figure 3.10	Failed Specimen	23
Figure 4.1	Liquid Limit Graph	26
Figure 4.2	Plasticity Chart	26
Figure 4.3	Gradation Curve	27
Figure 4.4	Compaction Curve	27
Figure 4.5	Load- Penetration Curve	28
Figure 4.6	UCS Graph	28
Figure 4.7	UCS Results of Set 1 (3 days cured)	29
Figure 4.8	UCS Results of Set 2 (3 days cured)	30
Figure 4.9	UCS Results of Set 3 (3 days cured)	30
Figure 4.10	UCS Results of Set 1 (7 days cured)	31
Figure 4.11	UCS Results of Set 2 (7 days cured)	31
Figure 4.12	UCS Results of Set 3 (7 days cured)	32

Figure 4.13	UCS Results of Set 1 (28 days cured)	32
Figure 4.14	UCS Results of Set 2 (28 days cured)	33
Figure 4.15	UCS Results of Set 3 (28 days cured)	33
Figure 4.16	Variation in UCS with increase in Sodium Oxide (3 days cured)	34
Figure 4.17	Variation in UCS with increase in Sodium Oxide (7 days cured)	35
Figure 4.18	Variation in UCS with increase in Sodium Oxide (28 days cured)	35
Figure 4.19	Variation in UCS with increase in Silica Modulus (3 days cured)	36
Figure 4.20	Variation in UCS with increase in Silica Modulus (7 days cured)	36
Figure 4.21	Variation in UCS with increase in Silica Modulus (28 days cured)	37
Figure 4.22	Formation of Efflorescence	37
Figure 4.23	Durability Test Results	38
Figure 4.24	Soaked CBR Results	39
Figure 4.25	Unsoaked CBR Results	39
Figure 4.26	Free Swell Index Valves	40
Figure 4.27	Flexural Strength Test Results	41
Figure 4.28	Input Data of IITPAVE	42
Figure 4.29	Locations of Critical Strain	42
Figure 4.30	Output data of IITPAVE	43
Figure 4.31	Pavement Cross-section	43

LIST OF TABLES

Table 2.1	Oedometer Test Results	7
-----------	------------------------	---

CHAPTER 1

INTRODUCTION

1.1 General

Engineers should utilize a suitable stabilizing strategy to obtain the required engineering properties due to excessive compressibility and low shear strength in soft soils (Saberian et al., 2020). Chemical stabilization is the most popular and traditional way of improving soft soils, with lime and Portland cement being the most commonly employed binders. The well-known pozzolanic and hydration reactions between calcium hydroxide alumina/silica and water enhance the strength. The ultimate products of such reactions are calcium aluminate hydrate, calcium aluminosilicate hydrate or calcium silicate hydrate, based on the amount of available silica and alumina (Bahmani et al., 2019).

Cement is the most often used binder in the building and road industries and its yearly production rate is expanding at an unprecedented rate. Cement producers produced 4.6 billion tonnes of cement globally in 2015. This figure is expected to rise to 4.83 billion tonnes by 2030 (Scrivener et al., 2018). This amount of production has several negative environmental consequences. For example, manufacturing one tonne of cement and one tonne of lime emits 0.95 & 0.79 tonnes of carbon dioxide and consumes 5000 & 3200 MJ of energy, respectively (Lemougna et al., 2018). Furthermore, cement production hastens natural resource depletion, consuming around 1.5 tonnes of limestone and clay for each tonne of cement produced (McLellan et al., 2011).

An amorphous precursor with a high alumina and silicate content reacts chemically with potassium or sodium-based activator to form geopolymers. (Bernal and Provis, 2014). Geopolymers are formed when a solid aluminosilicate material reacts with a highly concentrated aqueous alkali hydroxide or silicate solution. In the presence of alkali, alumina and silica gel polycondensates and forms an alkali aluminosilicate gel that acts as the binder. High hydroxyl concentration dissolves the impermeable aluminosilicate coatings on the surface of the precursor leading to further hydration and these hydration products aid in the improvement of properties (Thomas et al., 2018). Sodium hydroxide, sodium silicate or a combination of the two are the mostly utilized

activators for precursor activation in geopolymers. Researchers have demonstrated that this novel stabilization method has low to no carbon impact, significantly increases mechanical strength and controls volume change regardless of moisture level. The use of alkali activated materials is receiving more attention because of their promising properties like high compressive strength, outstanding resistance to fire and acid, rapid strength development and low shrinkage (Turner and Collins, 2013).

1.2 Relevance of the Study

In India, about 20 percentage of the area is covered with expansive soil. The growth of road transport in India is accelerating and there is a scarcity of land to satisfy the requirements. Furthermore, the expense of maintenance and rehabilitation of pavements built on these soils is rising daily. The safe disposal of fly ash, slag and other materials has been a difficult issue that requires an immediate solution due to the increasing influence of these pollutants on the environment and the harmful risk they offer to human health. However, cement production requires limestone and the rate at which we use cement is rising daily. One kg of carbon dioxide is released into the environment for each kg of cement produced. This increases the carbon footprint and poses a severe threat to the environment.

As a result, there is a requirement to discover an alternative binder that is both environmentally benign and dependent, such as cement. Therefore, this study justifies the usage of RHA, which has been alkali activated to stabilize BCS.

1.3 Objectives of the Study

- To ascertain the applicability of alkali activated RHA as a soil stabilizer.
- To improve the CBR, UCS, Durability, Flexural strength and swelling behaviour of BCS.
- To carry out the stress-strain analysis and design a flexible pavement using IITPAVE.

1.4 Organization of the Report

Before commencing the work, a detailed literature review was done and is presented in Chapter 2. Chapter 3 discusses the methodology of the work. Results and analysis of the work are shown in Chapter 4 and finally, Chapter 5 discusses the summary and conclusions reached at the end of the present work.

CHAPTER 2

LITERATURE REVIEW

2.1 General

The overview of soil stabilizing techniques and additives is explored in length in this chapter. Aluminosilicate precursors can be added in combinations or can be added alone. Fly ash and slag are the commonly used precursors. Fibers can also be added to enhance the strength further. This chapter explains the mechanism behind alkali activation and reviews different studies on this topic.

2.2 Alkali Activation Mechanism

The following stages are generally used to divide the alkali activation process: crystallization, polycondensation, condensation and dissolution (Duxson et al., 2007). These stages are briefly discussed below and are schematically represented in Fig. 2.1.

The initial reaction phase is the dissolution of the aluminosilicate component, which releases the reactive monomers silicate and aluminate. Bond dissociation in Al-O-Al and Si-O-Si occurs during dissolution, which happens only in a highly alkaline medium with a pH of more than 14 (Wu et al., 2019).

The colloidal phase begins with a process of water elimination due to a nucleophilic substitution reaction in which the elements silica and alumina hydroxide, which have an electric charge of -1, is linked to the others owing to OH group attraction of silicate with aluminate Al ions. This colloidal phase commences a process of chemical equilibrium known as condensation, which results in the formation of intermediate molecules. The production of an unstable aluminosilicate species at this point releases water molecules (Lahoti et al., 2019).

This action is repeated, with more water released and the production of the initial gels. The search for equilibrium continues, but load balancing is not impossible since aluminates and silicates both contain negative charges. The positive charge of alkali metal ions balances the charges of the generated unstable gels, prompting a rearrangement in the intermediate compound structure and initiating the synthesis of a more resistant final molecule. Then, the gel polycondensate, which might or might not crystallize and forms a stable gel. The material begins to harden, gaining other

recognized features of such activated alkali materials (Wu et al., 2019). Figure 2.2 shows the formed geopolymer network.

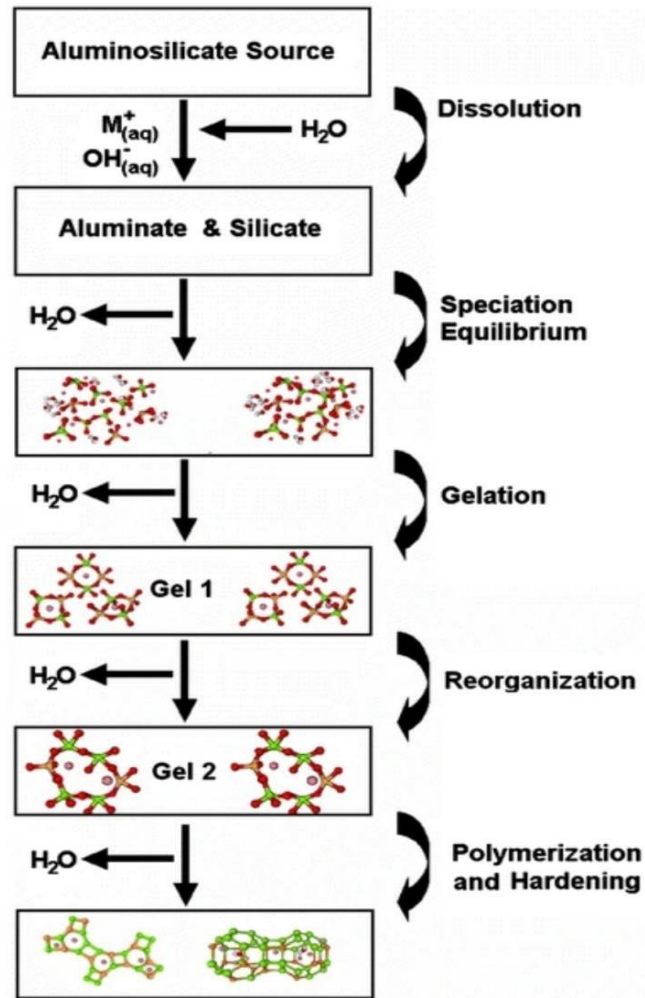


Figure 2.1- Flow Chart of Alkali Activation

(Source: Duxson et al., 2007)

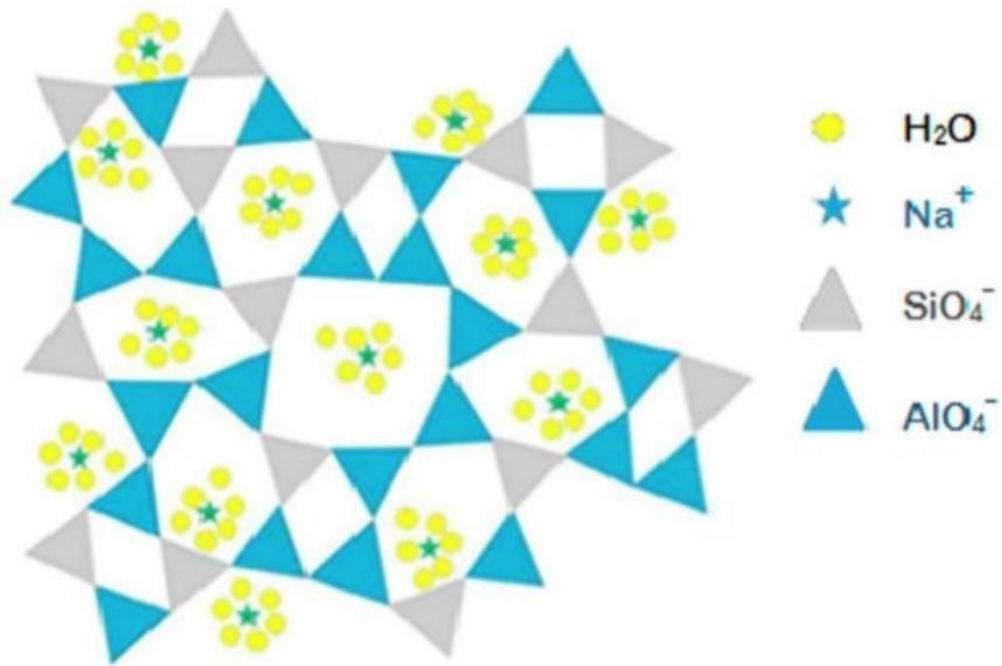


Figure 2.2- Formed Geopolymer Network

(Source: Lahoti et al., 2019)

2.3 Combination of Precursors

2.3.1 Volcanic Ash and Slag

Miraki et al. (2021) did a Scanning Electron Microscopy (SEM) analysis and noticed the development of N-A-S-H (sodium silica hydrate) gel in the correct proportions of volcanic ash and slag, accounting for a rise in strength. Replacing volcanic ash with slag resulted in lesser values of the carbon index, indicating that samples containing more slag and a lesser proportion of ash are more sustainable.

2.3.2 Fly Ash and Slag

Amulya et al. (2018) carried out an analysis to stabilize lithomargic clay with varying amounts of fly ash and slag. According to experimental results, there is a 30-40% rise in UCS for stabilized soil. Alkali activated samples passed all Wetting Drying (WD) cycles, indicating that the soil has high durability and could be utilized in the pavement base layer.

2.3.3 Slag and Paper Sludge Ash

Mavroulidou et al. (2021) investigated the effect of potassium hydroxide and a variety of alkali salts in stabilizing clay and silty soils. The studied alkali activated cement mixtures improved UCS and stiffness while decreasing swelling tendency. Alkali activated cement with potassium hydroxide had the highest strength and stiffness. Paper Sludge Ash (PSA) added clayey soil had significant strength increase and PSA added samples demonstrated good performance in WD cycles. Oedometer test outcomes are shown in Table 2.1.

Table 2.1- Oedometer Test Results
(Source: Mavroulidou et al., 2021)

Soil mix	Volumetric swelling strain (%)	Compression index
Untreated silt	2.3	0.08
Silt+6% Na ₂ SiO ₃ +10% Slag	0.01	0.07
Silt+6% K ₂ CO ₃ +10% Slag	0.9	0.07
Silt+6% KOH+10% Slag	0.04	0.02
Untreated Clay	28.1	0.49
Clay+10% PSA	0.16	0.02
Clay+6% PSA+10% Slag	0.15	0.06
Clay+6% Na ₂ SiO ₃ +10% Slag	0.15	0.1
Clay+6% PSA+3% Na ₂ SiO ₃ +15% Slag	0.02	0.06
Clay+6% K ₂ CO ₃ +10% Slag	2.8	0.19
Clay+3% PSA+3% K ₂ CO ₃ +10% Slag	0.08	0.025

2.3.4 Calcium Carbide Residue and Fly Ash

Phetchuay et al. (2016) examined the strength increase in clay by adding fly ash and calcium carbide residue. Higher fly ash content necessitates a higher amount of sodium hydroxide for leaching. Thus, the sodium hydroxide/silicate ratio decreases with a rise in fly ash. This rise in the liquid/fly ash ratio initially enhances the UCS. However, if liquid/fly ash exceeds the optimal value, the strength falls because precipitation occurs at an early stage even before the polycondensation process.

2.3.5 Slag, Fly Ash and Ordinary Portland Cement

Chen et al. (2020) worked on soft clayey soil stabilization by adding lime, fly ash and Portland cement with sodium hydroxide and silicate. The compressive strength of stabilized samples rose considerably with increased curing days and alkali activated binder amount, but the UCS of untreated specimens did not improve. The presence of calcium silica hydrate paste in SEM analysis is advantageous for forming a denser microstructure. Hydraulic conductivity values decreased with the addition of alkali activated binder, as shown in Figure 2.3.

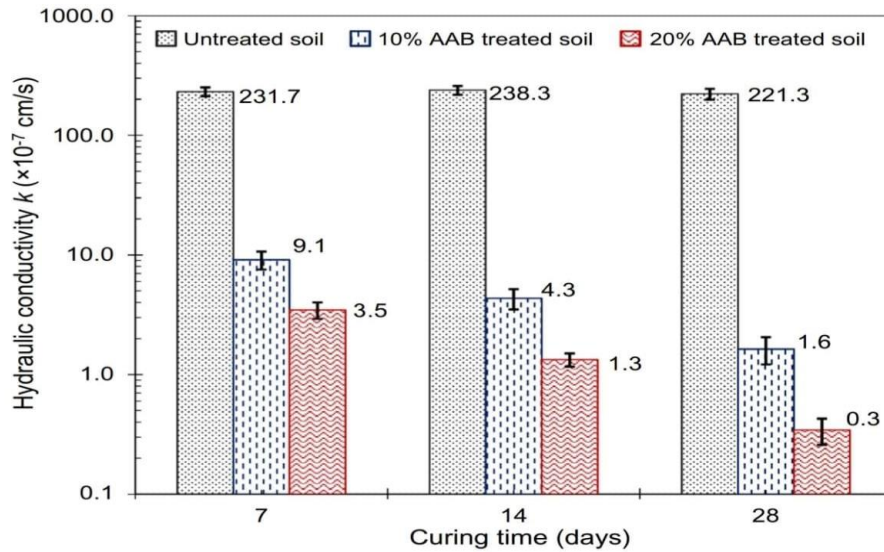


Figure 2.3- Hydraulic Conductivity Results

(Source: Chen et al., 2020)

2.3.6 Slag and Fly Ash (added with construction and demolition waste)

Abhilash et al. (2020) carried out research on four types of prepared clayey soil samples. Cement, ground granulated blast furnace slag, demolition, and construction waste were mixed with soil in the first type. In the second type, cement was replaced with lime. In the third and fourth mixes, slag and fly ash have been replaced by cement and lime, respectively. Sodium hydroxide was also used in the third and fourth mixes for the alkali activation. In terms of achieved strength, the lime stabilized mix was found to be the least effective. Strength was lesser than cement stabilized mix. In alkali activated samples, fly ash stabilized samples were more effective.

2.4 Addition of Fibers

A variety of fibers, like polypropylene fibers, glass fibers, coir fibers, hemp fibers etc., can be added to alkali activated samples to further enhance the strength.

2.4.1 Fly ash, Slag and Polypropylene Fibers/Glass Fibers

Mazhar et al. (2020) added slag and fly ash together in BCS. Alkali activators used are sodium hydroxide and silicate. Polypropylene fibers and glass fibers were also added separately to the samples. The UCS and indirect tensile strength of the stabilized BCS were enhanced by approximately 65 percent and 48 percent, respectively. Furthermore, the strength in shear of the fiber and slag-added soil was greater than that of fly ash-fiber in both fiber-alkali activated binder soil samples.

2.4.2 Fly Ash and Coir Fiber

Tan et al. (2020) examined the effectiveness of Class-C fly ash-treated clayey soil that is reinforced with treated and untreated fibers of coir by using potassium hydroxide. The Class-C fly ash added with a treated fiber combination has the highest CBR value. According to the atomic force microscopy data, higher UCS with treated fiber is mainly owing to its excellent packing efficacy in filling pores. It provides compelling evidence that Class-C fly ash added with treated fibers improves the soil strength. The treated fiber-added mixture has the best UCS value, 35% higher than a comparable mixture without fibers.

2.4.3 Fly ash, Slag and Coir Fibers/Hemp Fibers

Syed et al. (2021) examined the efficiency of slag and fly ash in clayey soil like BCS. Coir fibers and hemp fibers have been added separately to the samples. The values of the subgrade strength indicators like CBR and resilient modulus rose by approximately 55% and 38%, respectively. An equation for the prediction of CBR for the treated soil was suggested.

2.5 Slag as Precursor

Thomas et al. (2017) examined the maximum dry density and optimum moisture content values on specimens stabilized with slag, enzyme and cement respectively. The cohesiveness of the treated soil rose substantially. The UCS and shear strength values of slag-treated samples

outperformed those of the Ordinary Portland cement stabilized soil. Variation in the shear strength parameter is shown in Fig. 2.4.

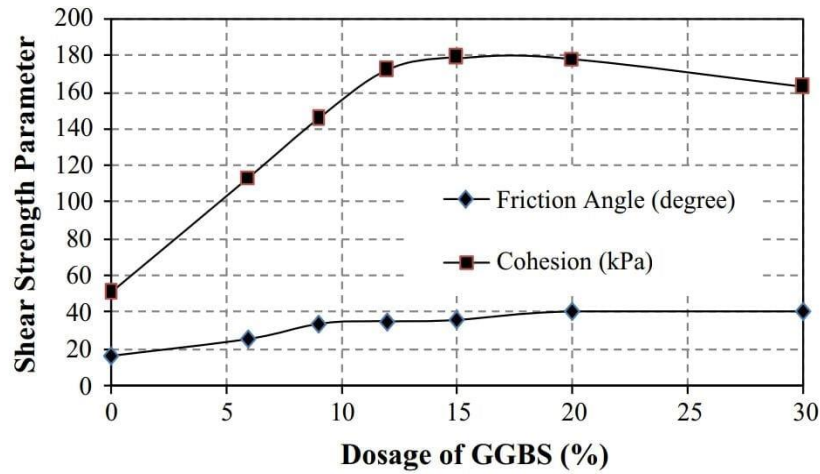


Figure 2.4- Shear Strength Parameter Variation

(Source: Thomas et al., 2019)

Lang et al. (2020) studied the strength development in clay along with dredged sludge that has been stabilized using ground granulated blast furnace slag, which was alkali activated. When optimal UCS was compared under the same activator dose, composite activators were more efficient than single activators in activating ground granulated blast furnace slag to acquire greater stabilized dredged sludge strength. It was suggested that a 20% sodium silicate/hydroxide ground granulated blast furnace slag binder could be utilized. The experimentally derived linear empirical equations were used to estimate the 60 and 90 days UCS of alkali activated slag stabilized dredged sludge by using the known 28 days UCS.

Du et al. (2016) added slag, which was activated with magnesium oxide to stabilize kaolin clay. When subjected to the WD cycle, the slag-stabilized kaolin clay showed greater dry density while exhibiting reduced loss in mass than the cement-stabilized samples. Variation in mass loss is shown in Figure 2.5. The pH of the slag-stabilized clay and cement-stabilized samples fell as the WD cycle increased. UCS test results of slag-stabilized kaolin clay showed 1.5 times higher strength than cement-stabilized samples and the change of UCS is represented in Fig. 2.6.

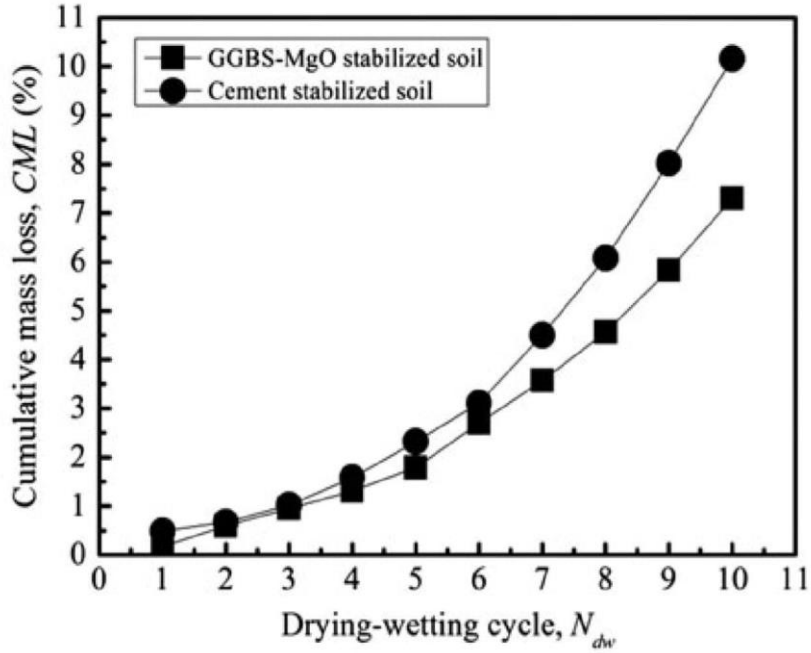


Figure 2.5- Variation in Mass Loss

(Source: Du et al., 2016)

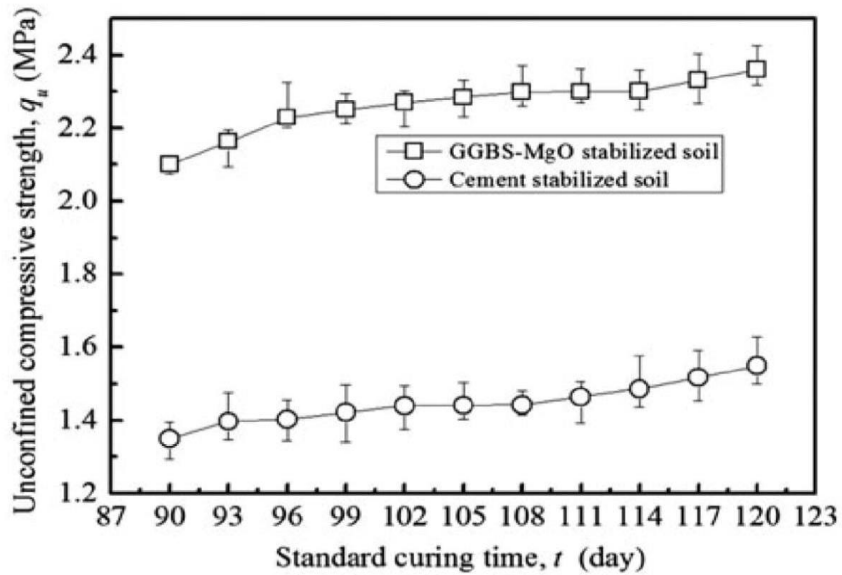


Figure 2.6- Variation in UCS

(Source: Du et al., 2016)

2.6 Fly Ash as Precursor

Murmu et al. (2019) stabilized BCS by separately adding fly ash of particle size 75 microns and 425 microns, with and without using alkali. The geopolymer-stabilized BCS has significantly increased UCS. Both samples are equally efficient in lowering swelling and shrinkage values. Variation in the free swell ratio is shown in Figure 2.7.

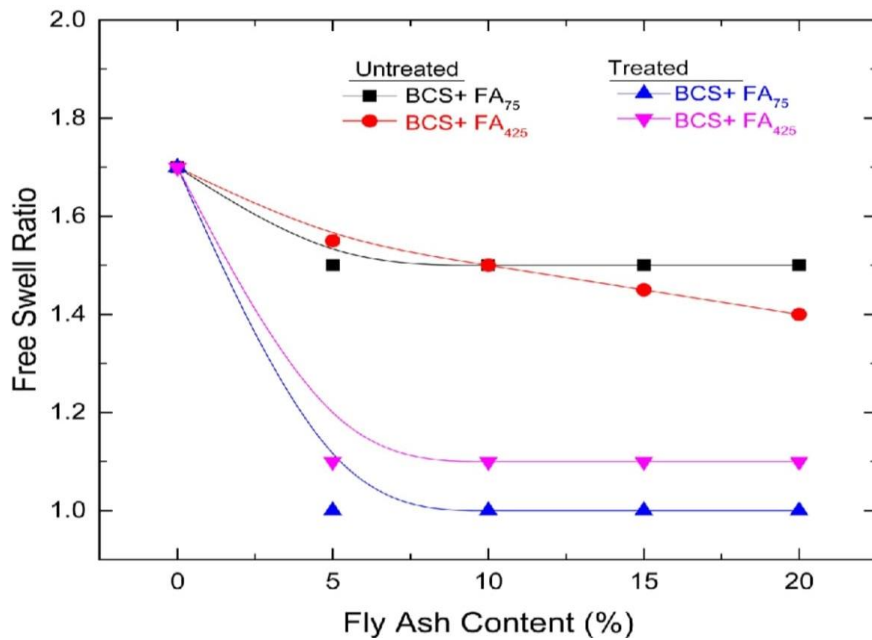


Figure 2.7- Variation in Free Swell Ratio

(Source: Murmu et al., 2019)

Syed et al. (2020) also studied the suitability of fly ash to stabilize clay soil. Fly ash was added to stabilize BCS by using conventional activators. Plasticity and swelling index was significantly reduced in the treated BCS samples. There was a reduction in volumetric instability (swell/shrink) by encasing the particle in a thin cementitious gel surface. The CBR value was significantly improved with BCS treatment using an alkali activated binder.

2.7 Analysis of Pavement in IITPAVE

With technological developments, the use of software to study pavement behaviour has increased significantly. Software can be used to investigate pavement behaviour under various loads, climatic and environmental conditions. For flexible pavement analysis, free software such as KENPAVE, IITPAVE, ILLIPAVE, MICH PAVE, Pave Xpress and commercial software such as Infra work software, MXROAD, PAVERS, Street Pave and AASHTOWare are available (Visvanathan et al., 2020).

Mohan and Kumar (2020) did a research to analyze flexible pavement using IITPAVE software. Flexible pavements were constructed in compliance with IRC 37-2012 utilizing data from traffic field investigations and the CBR values of subgrade soil. The research was conducted with IITPAVE software. The study focused on the NH-234 Madhugiri-Chikkaballapur stretch. The findings revealed that the actual values for horizontal tensile strain and vertical compressive strain were less than the allowed ranges. Therefore, the design is reliable and the assumed pavement thickness is correct. In a study conducted by Harish (2017) to analyze the pavement design in IITPAVE, he employed cementitious and recycled asphalt materials. Bangalore was chosen as the research location. After the subbase had been designed using cementitious material, IITPAVE was utilized to analyze it. The software was used to draw a comparison between the cementitious subbase and the conventional subbase. The usage of cementitious material improved the effectiveness of the pavement.

2.8 Closure

According to the aforementioned literature review, subgrade soil can be stabilized using various precursors to enhance its engineering properties. Effects of different precursor combinations and fiber addition in enhancing the soil strength were discussed. The efficacy of fly ash and slag as precursors in stabilizing soil was also reviewed. The strength and durability of the alkali activated soil specimens were found to be high. Based on the gaps in the literature review, the current work focuses on the utilization of alkali activated RHA in the stabilization of BCS.

CHAPTER 3

METHODOLOGY

3.1 General

Different studies on the application of aluminosilicate materials together with alkalis to improve soil properties were discussed. This chapter mainly deals with sample collection, preliminary tests, specimen preparation, laboratory investigation and pavement design using IITPAVE.

3.2 Detailed Methodology

The general methodology followed in this study is shown in Figure 3.1 below.

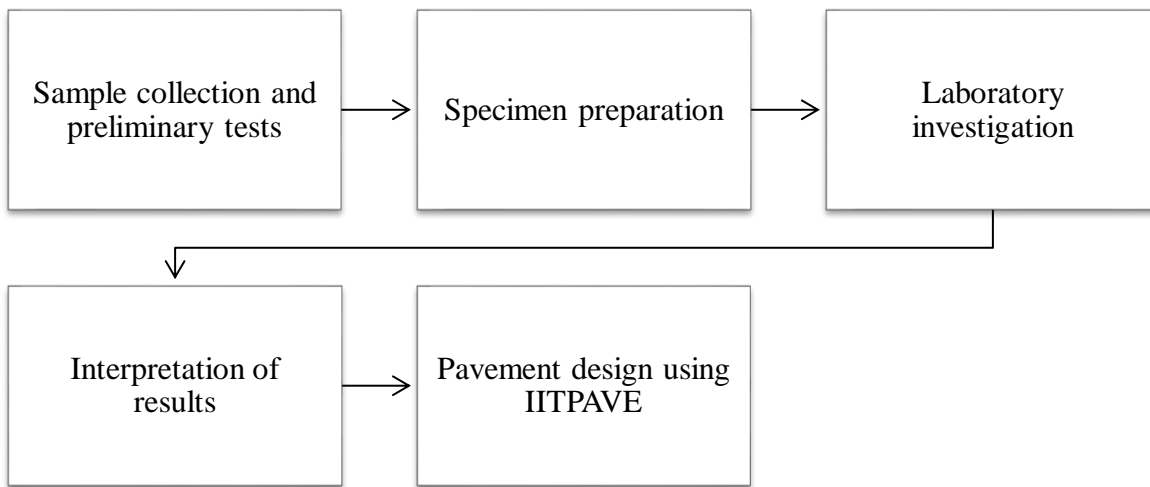


Figure 3.1- Methodology Flow Chart

3.3 Sample Collection and Preliminary Tests

For the current work, BCS was collected from Chittur taluk in the Palakkad district. RHA was collected from the Royal rice mill located in the district of Alappuzha and was burnt in a furnace at a temperature of 600°C. Sodium silicate was purchased online in liquid form and sodium hydroxide (pellets) was obtained from the material testing laboratory of TKM College of Engineering. The preliminary tests were the Hydrometer Analysis, Atterberg Limits Test, Swelling Test, Proctor Compaction Test, Unconfined Compression Test and CBR Test.

3.4 Specimen Preparation

For the present study, RHA was added at 5%, 10%, 15% and 20% to the BCS. Sodium silicate and hydroxide are the alkalis used. As far as alkali activation is concerned, many parameters can affect the strength characteristics. Here, sodium oxide (Na_2O) and silica modulus (M_s) were chosen as the parameters that will be varied (Amulya and Ravi Shankar, 2020). Silica modulus is the ratio of silica oxide and sodium oxide. Sodium oxide was added at 2%, 3% and 4% of RHA. Silica modulus was varied in the ratios 0.5, 1 and 1.5 and the water/binder ratio was taken as 0.25 (Amulya and Ravi Shankar, 2020). Different sample combinations are shown in Figure 3.2, where RHA x represents different percentages of RHA, SO y represents different percentages of sodium oxide and SM z represents different values of silica modulus. In total, there are 36 combinations. For all the tests, three samples were cast for each combination and the average value was taken.

		SO 2-SM 0.5
		SO 2-SM 1
		SO 2-SM 1.5
		SO 3-SM 0.5
5%,10%,15%,20% RHA	+	SO 3-SM 1
		SO 3-SM 1.5
		SO 4-SM 0.5
		SO 4- SM 1
		SO 4- SM 1.5

Figure 3.2- Sample Combinations

The mix was prepared by first mixing the BCS and RHA thoroughly. RHA was sieved through the 75-micron sieve. The calculated amount of sodium hydroxide pellets was dissolved in water. After that, it was mixed with the estimated amount of sodium silicate and kept overnight for the reaction. It was mixed with the mixture of BCS and RHA and specimens were prepared at optimum moisture content. Figure 3.3 and Figure 3.4 shows the RHA and chemicals used for the study, respectively.



Figure 3.3- RHA Used for the Study

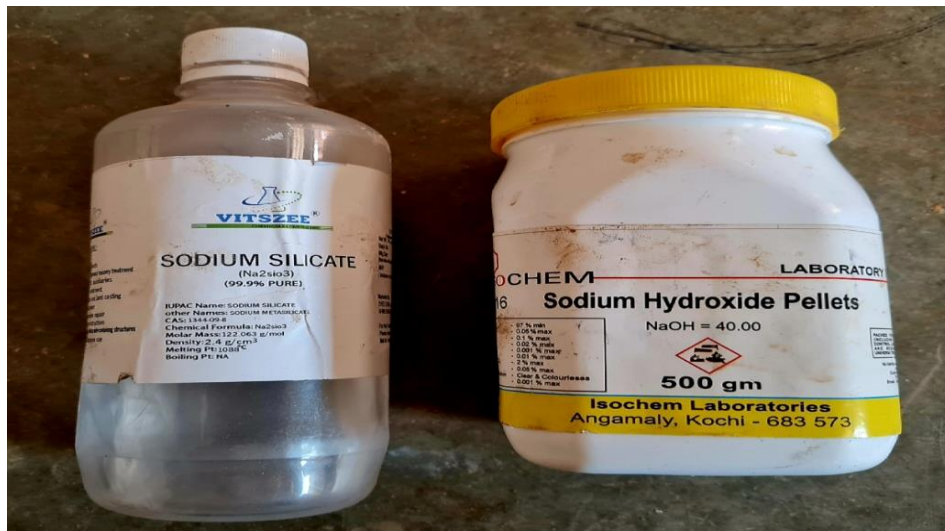


Figure 3.4- Chemicals Used for the Study

3.5 Laboratory Tests

Figure 3.5 shows the soil used for the study. Several preliminary tests were done on the soil sample to characterize the soil type. Hydrometer Analysis, Atterberg Limits Test, Swelling Test, Proctor Compaction Test, Unconfined Compression Strength Test and CBR Test were done as part of the

preliminary analysis. Unconfined Compression Strength Test, Durability Test, CBR Test, Swelling Test and Flexural Strength Test were performed on stabilized soil samples.



Figure 3.5- Soil Used for the Study

3.5.1 Liquid Limit Test (IS 2720: Part 5: 1985)

The test was carried out using soil that had passed through a 425-micron sieve. A tray was filled with 200 grams of soil and water was mixed into the soil. The soil paste was spread inside the Casagrande apparatus. A cut was created in the centre of the soil using a groove. After giving some rotations, the two sections will come together. Take a small amount of it and determine the moisture content. Make a note of the number of blows. The amount of moisture equivalent to 25 blows is the liquid limit.

3.5.2 Plastic Limit Test (IS 2720: Part 5: 1985)

The soil was sieved through a 425-micron IS sieve to determine its plastic limit. 25 grams of soil was mixed adequately with distilled water until it became plastic enough to be rolled into a ball easily. With fingertips, the ball was rolled against a glass plate. The spherical form changes to a thread shape of 3 mm diameter. Repeat the technique until the thread 3 mm in diameter shows signs of crumbling. Place the soil in the container to examine the moisture content. The soil plastic limit is the moisture content at which soil threads reveal fractures.

3.5.3 Proctor Compaction Test (IS 2720: Part 7: 1983)

It is a commonly used laboratory test for soil compaction. A 2.5 kilogram weight dropped from a 30 centimeter height compacts the soil in 5 layers with 25 blows in each layer. The test is performed for different moisture content to identify the moisture content at which the dry unit weight value is maximum. The Proctor Compaction Test is done to obtain the optimum moisture content and dry density values.

3.5.4 CBR Test (IS 2720: Part 16: 1987)

It is done to evaluate the structural integrity of flexible pavements and subgrade. Values of CBR are measured at 2.5 & 5mm penetrations. CBR is defined as the ratio of the force required per unit area to enter a mass of soil at 1.25 mm/min to the force necessary to enter a standard material at the same rate. Figure 3.6 shows the preparation of CBR specimens.



Figure 3.6- Preparation of CBR Specimens

3.5.5 Hydrometer Analysis (IS 2720: Part 4: 1985)

A hydrometer can be used for particle size analysis by transferring approximately 50 grams of oven-dried soil that passes via a 75-micron sieve to an evaporating dish. The soil was treated with

sodium hexametaphosphate. Water was used to create the slurry. The soil was then placed into a dispersion cup and swirled for 15 minutes. The suspension was then transferred into a 1000ml standard measuring flask and mixed thoroughly. A stopwatch is started and the jar is kept on a table. The hydrometer is put into the suspension, and the first reading is obtained 30 seconds after the sedimentation begins. Further readings are collected at 1, 2, 4, 8, 15, and 30 minutes. The hydrometer was withdrawn from the jar, cleaned with distilled water and floated in a distilled water comparison cylinder and further readings were recorded.

3.5.6 Unconfined Compression Strength Test (IRC 2720: Part 10: 1991)

It is a triaxial test modification in which unconfined pressure is kept at zero. Unconfined compression test equipment is used in this test and a soil sample is placed on the equipment. The dial gauge and proving ring are set at zero and compressive load is given to the specimen. The compressive force is calculated using the proving ring measurement and the axial strain is calculated using the dial gauge reading. The stress value is computed by dividing the force by area. A stress-strain graph is plotted and UCS is found. Figure 3.7 shows the casted specimens.



Figure 3.7- Casted Specimens for Compression Test

3.5.7 Swelling Test (IS 2720: Part 41: 1977)

Free swell index is the volume rise in soil that takes place when it is immersed in water. Take two 10 grams of pulverized soil samples and oven-dry them after passing them through a 425-

micron IS sieve. Fill two graduated glass cylinders with these two specimens. Fill one cylinder with distilled water and another with kerosene oil to the 100ml mark. Release trapped air by gently shaking or agitating the container with a glass rod. Let the suspension reach an equilibrium condition. The soil volume is noted and the free swell index is calculated using Equation 3.1. Figure 3.8 shows the swelling test on the soil.

$$\text{Free swell index (\%)} = \frac{v_d - v_k}{v_k} \times 100 \quad (3.1)$$

Where,

v_d - Reading of soil sample volume in the water-filled cylinder

v_k - Reading of soil sample volume in the kerosene-filled cylinder



Figure 3.8- Swelling Test on Soil

3.5.8 Durability Test (ASTM 559D)

Throughout years of exposure, the road material durability must sustain stability, integrity and bond with the soil despite cyclic weathering modification and severe traffic conditions. The durability test involves WD tests performed on cylindrical samples cast on UCS mould. The WD test has been conducted and the samples have been soaked in water for 5 hours before being oven dried at 71 degrees Celsius for 42 hours. Each soaking and drying of a sample is referred to as a cycle. The weight loss at each cycle would be recorded. After the 12 cycles, the weight reduction should not surpass 14%. Figure 3.9 shows the sample immersed in water.

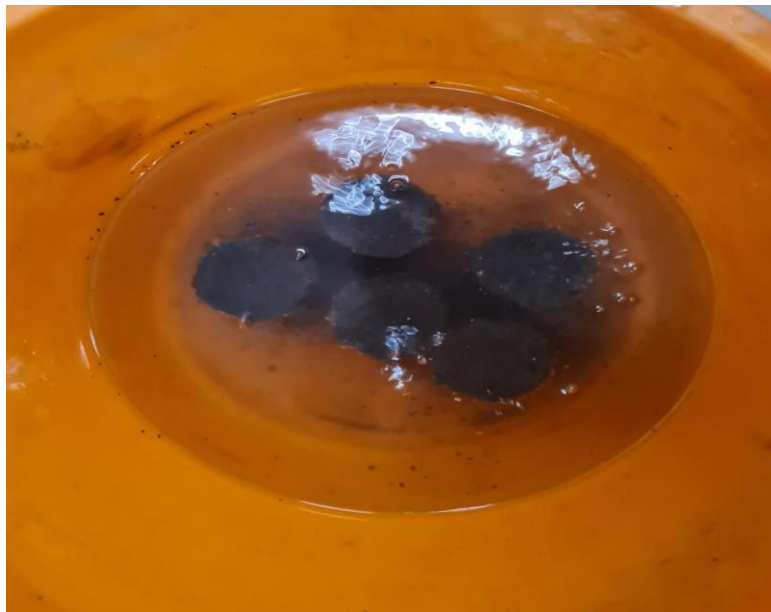


Figure 3.9- Soil Immersed in Water

3.5.9 Flexural Strength Test (IS 4332: Part 6: 1972)

The test is done on a multi-frame digital testing machine. Soil beams of 28 cm x 7.5 cm x 7.5 cm were cast for the experimental study. The maximum load was recorded under two-point loading and by using Equation 3.2, the modulus of rupture (M_R) was calculated. Figure 3.10 shows the failed specimen.

$$M_R = \frac{Pl}{bd^2} \quad (3.2)$$

Where,

P - Breaking load

l - Sample length

b - Sample breadth

d - Sample depth



Figure 3.10- Failed Specimen

3.6 Pavement Design in IITPAVE

The mechanistic-empirical program called IITPAVE software is utilized for flexible or bitumen pavement design and analysis. Pavement design is done on this software based on IRC 37-2018. The Poisson's ratio, elastic modulus, the thickness of various layers, vehicle tire pressure and wheel

load are the input variables used to achieve stresses and strains at various layers. The outputs obtained are stress, strain and deflection. Here the study is concentrated on subgrade soil and hence the focus is on vertical compressive strains acting on the top layer of subgrade. The pavement section is considered as a layered system. The linear layered elastic modulus is utilized to calculate stresses along with strains at critical locations. Resilient modulus is regarded as the ideal input for linear elastic theory for the analysis of flexible pavement, which is measured in repeated load tests with only accounting for the elastic component of the specimen deformation.

In the analysis, effective CBR and design traffic is found and a trial section is selected. The resilient modulus for the granular layer is calculated and the resilient modulus value of the bituminous course will be taken from IRC 37-2018. The granular base and subbase layer are taken as a single layer and are assigned a single modulus value for the analysis. Allowable strains in the critical locations (top layer of subgrade and bottom of bituminous layer) will be found and if it is lesser than the actual strain, then the pavement is safe. If not, it needs to be redesigned

3.7 Closure

The test protocol employed for the study includes the conduction of the UCS Test, CBR Test, Swelling Test, Flexural Strength Test and Durability Test. Based on UCS and Durability Test findings, the selected specimens were subjected to the CBR Test, Flexural Strength Test, Swelling Test and IITPAVE analysis. The results obtained will be evaluated to identify and choose the best combination that gives the best results in subgrade stabilization.

CHAPTER 4

RESULTS AND ANALYSIS

4.1 General

Before excavating, the topsoil layer at a depth of 15 cm was removed because it will have natural vegetation on top. The soil was obtained at a depth of 15 cm for the investigation. Field moisture content was observed to be 21.22% and specific gravity was found to be 2.7. Soil has a free swell index of 38.2%. Other Preliminary tests were also done and after the preliminary tests, samples were prepared using the stabilizers and subjected to various tests, as mentioned earlier. The test results have been compared and inferred to evaluate the efficacy of the stabilizer on the soil characteristics.

4.2 Preliminary Tests

Preliminary tests performed on the soil were Hydrometer Analysis, Proctor Compaction Test, Atterberg Limits Test, UCS Test & CBR Test.

4.2.1 Atterberg Limits

The liquid limit and plastic limit of the soil sample were found to be 55% and 27%, respectively. Therefore, the sample is highly plastic. The plasticity index obtained was 28. The soil was classified as clay of high compressibility (from the plasticity chart). The liquid limit graph and plasticity chart are shown in Figure 4.1 and Figure 4.2, respectively.

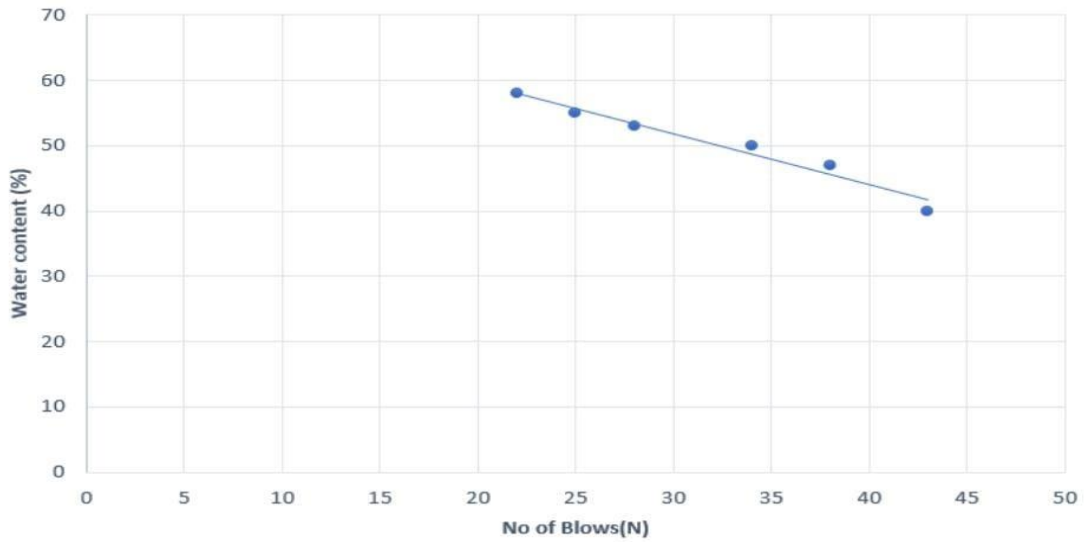


Figure 4.1- Liquid Limit Graph

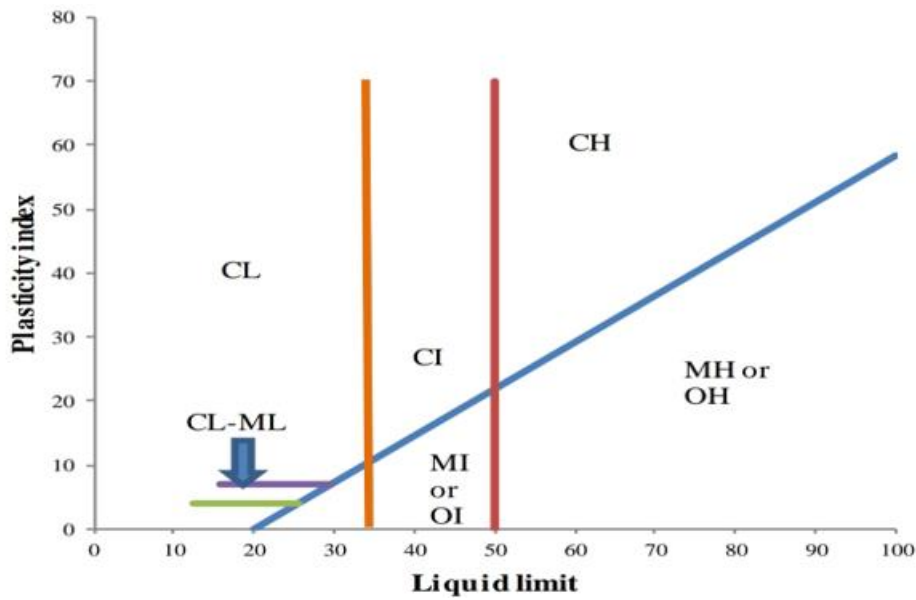


Figure 4.2- Plasticity Chart

4.2.2 Sieve Size Analysis

Figure 4.3 shows the gradation curve. Collected soil has 67% clay, 29% silt and 4% sand particles.

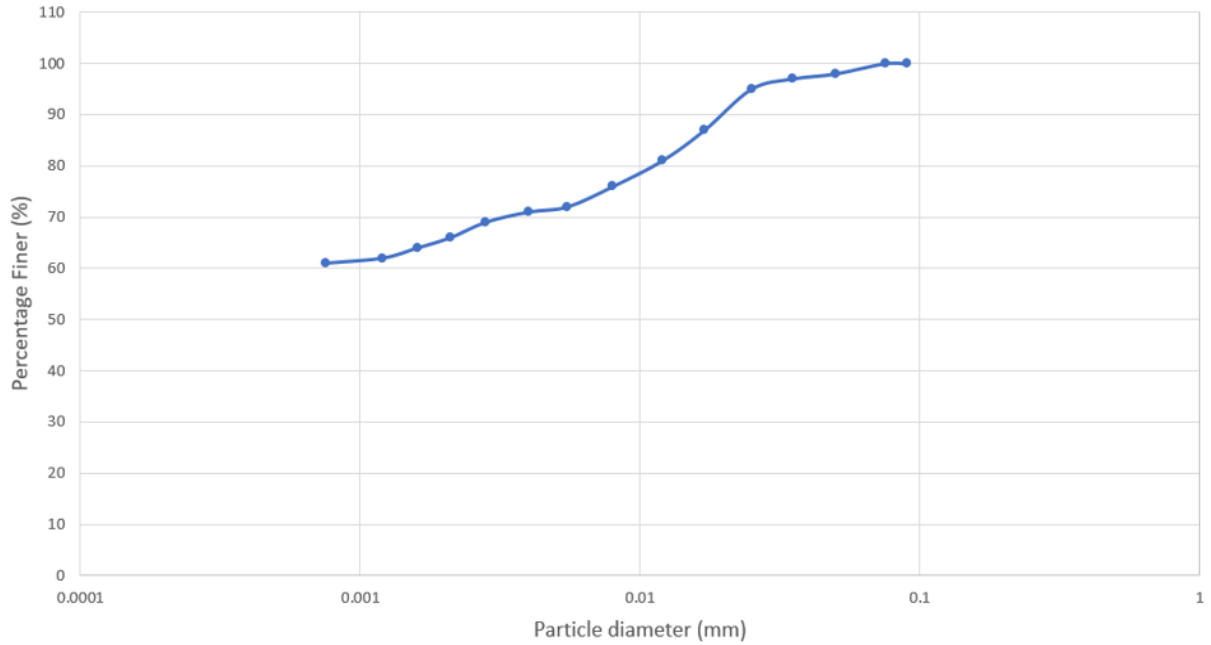


Figure 4.3- Gradation Curve

4.2.3 Proctor Compaction Test

The optimum moisture content was found to be 20% and the maximum dry density is 1.58 g/cc.

Figure 4.4 shows the compaction curve.

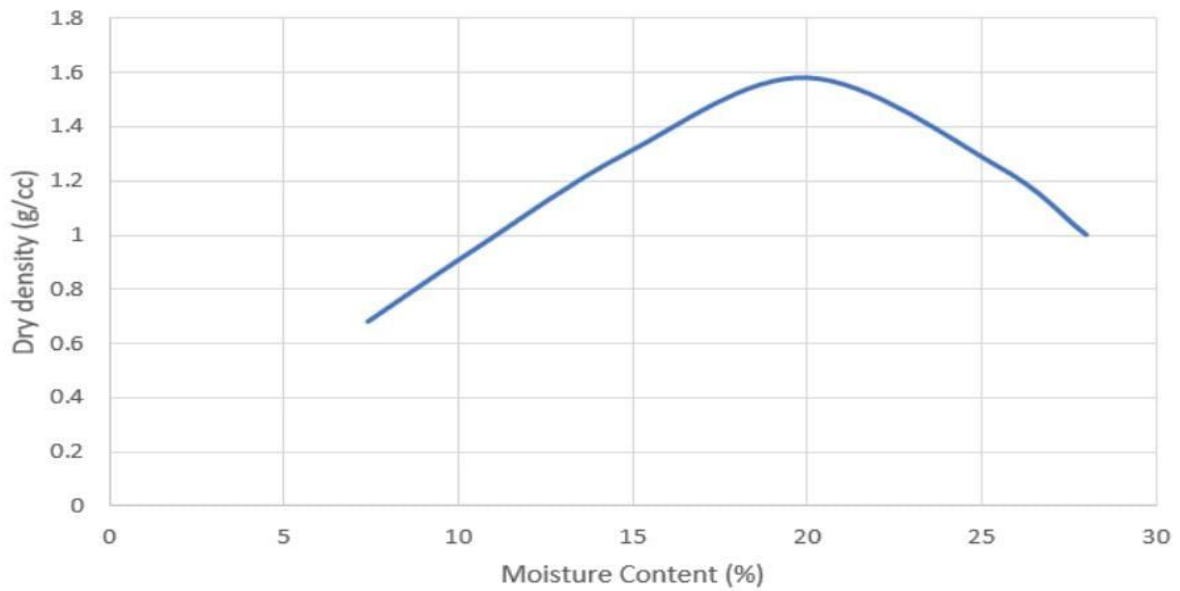


Figure 4.4- Compaction Curve

4.2.4 CBR Test

CBR for 2.5 mm penetration was found to be 2.3%. The load-penetration curve is shown in Figure 4.5.

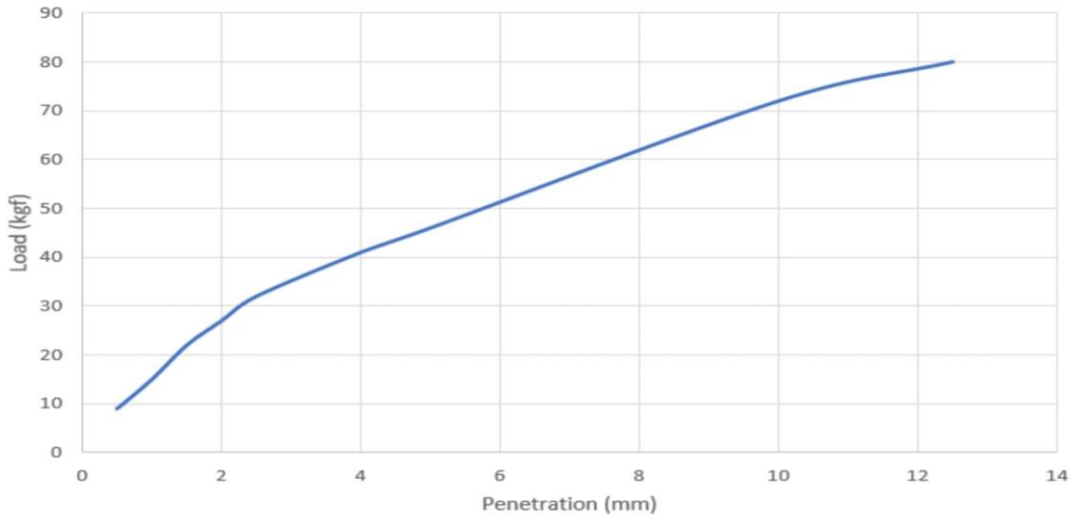


Figure 4.5- Load-Penetration Curve

4.2.5 Unconfined Compression Strength Test

UCS has been observed to be 0.72 kg/cm^2 (72 KPa). UCS graph is shown in Fig. 4.6.

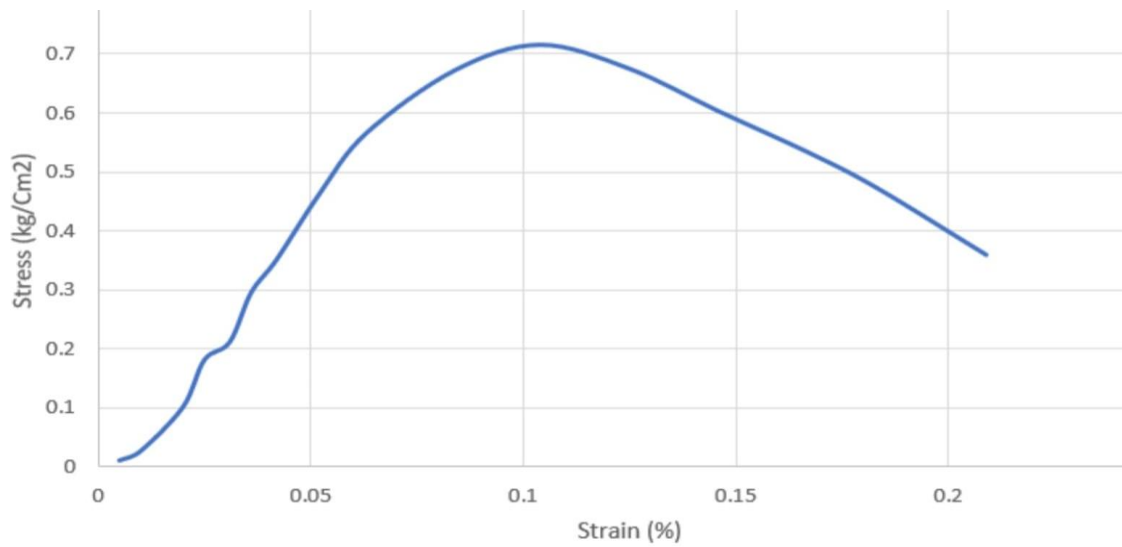


Figure 4.6- UCS Graph

4.3 Laboratory Tests on Stabilized Soil Samples

Unconfined Compression Strength Test, Durability Test, CBR Test, Flexural Strength Test and Swelling Test were done on stabilized samples.

4.3.1 Unconfined Compression Strength Test

This test was done on all 36 combinations after curing the specimens for 3, 7, and 28 days. The UCS value of raw BCS was 72 KPa. Soil samples with sodium oxide content two percentage is considered as set 1, soil samples with sodium oxide content three percentage is considered as set 2 and soil samples with sodium oxide content four percentage is considered as set 3. In Figures 4.7, 4.8 and 4.9, the results of 3 days cured samples are shown. Figures 4.10, 4.11, 4.12 and 4.13, 4.14, 4.15 show the results of 7 and 28 days cured samples, respectively. It was observed that with an increase in RHA content from 5% to 20%, the compressive strength increases because of the greater availability of the aluminosilicate material (Murmu et al., 2019). Sample RHA 20-SO 4-SM 0.5 has the highest compressive strength value.

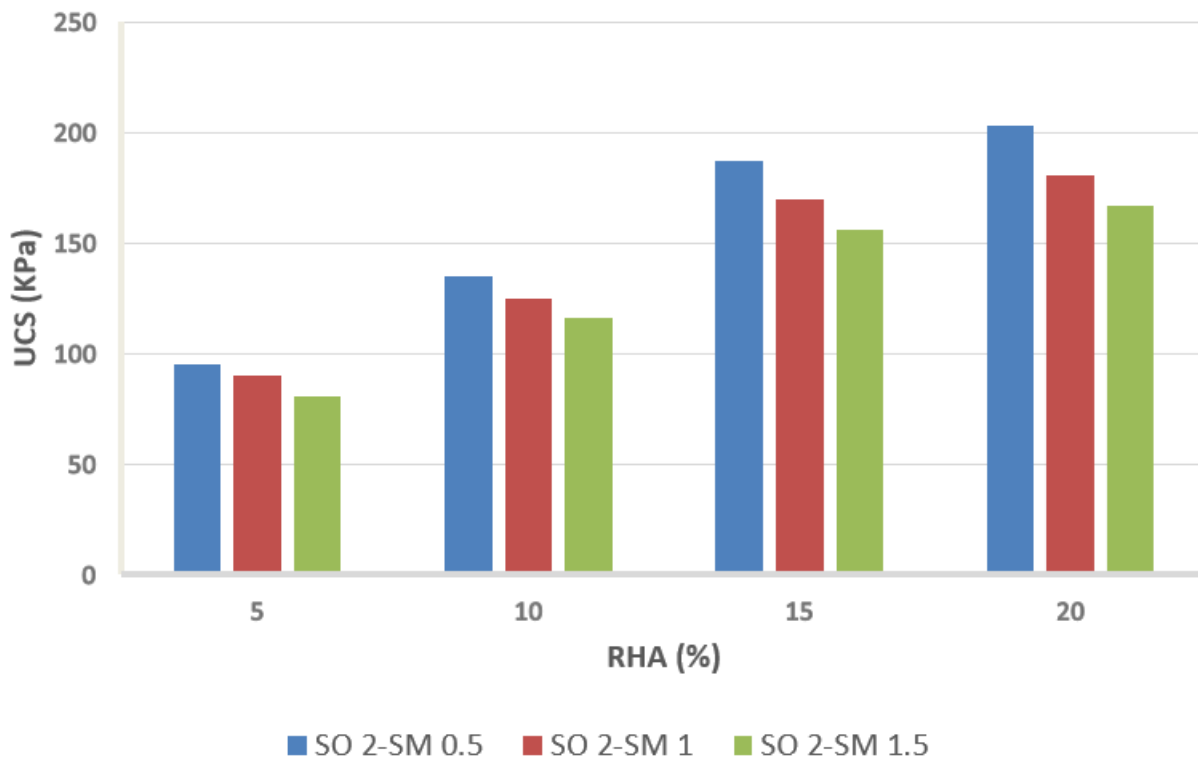


Figure 4.7- UCS Results of Set 1 (3 days cured)

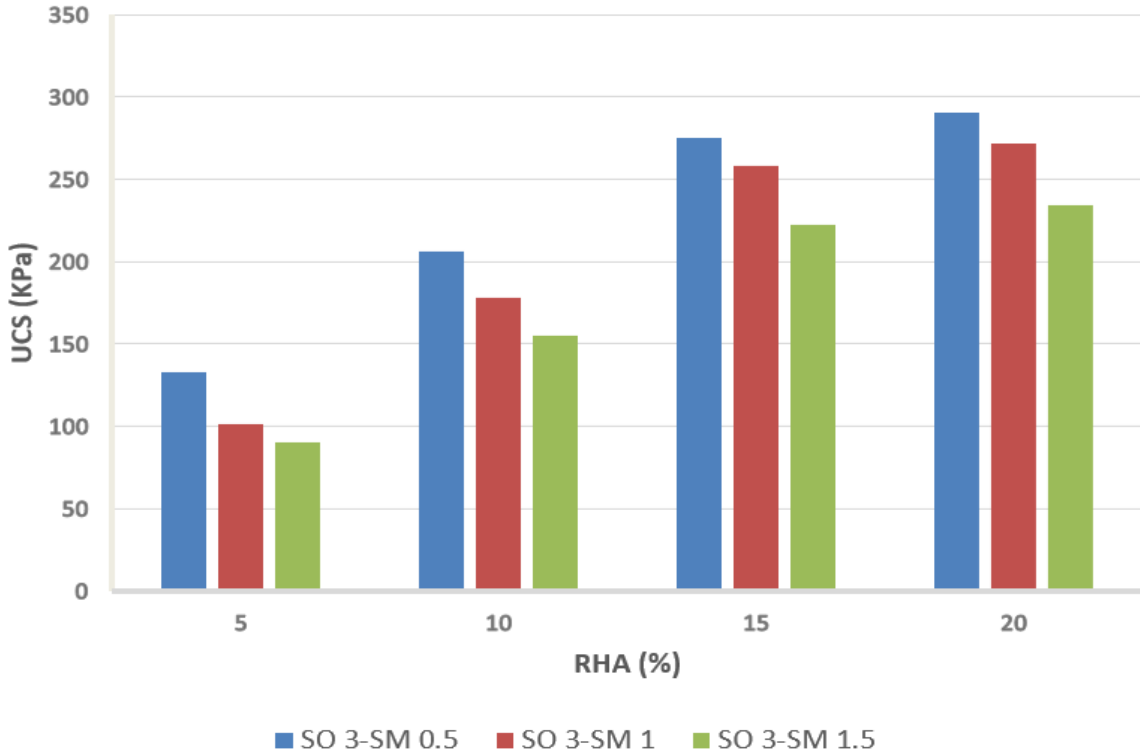


Figure 4.8- UCS Results of Set 2 (3 days cured)

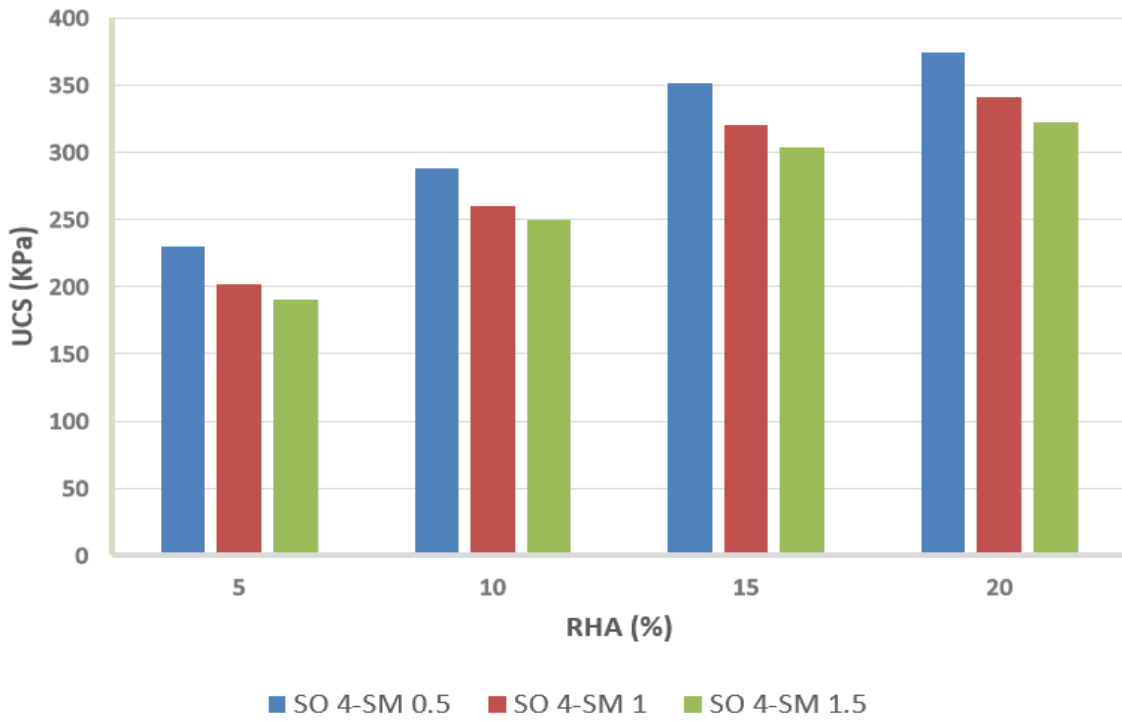


Figure 4.9- UCS Results of Set 3 (3 days cured)

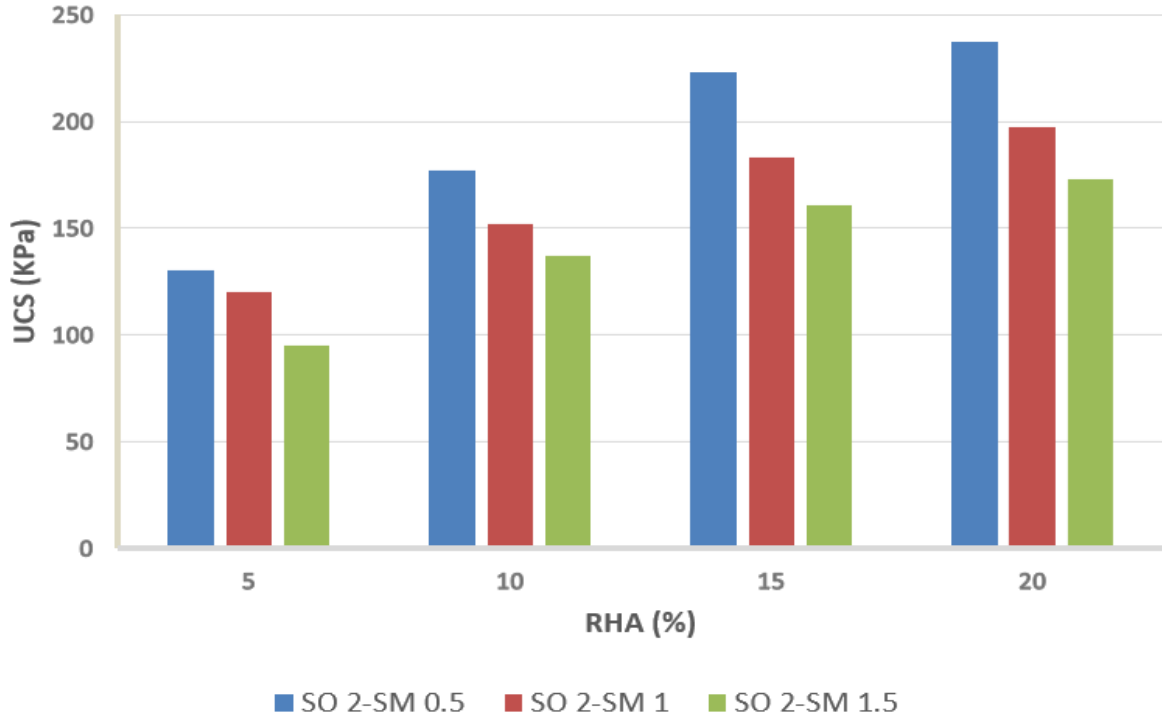


Figure 4.10- UCS Results of Set 1 (7 days cured)

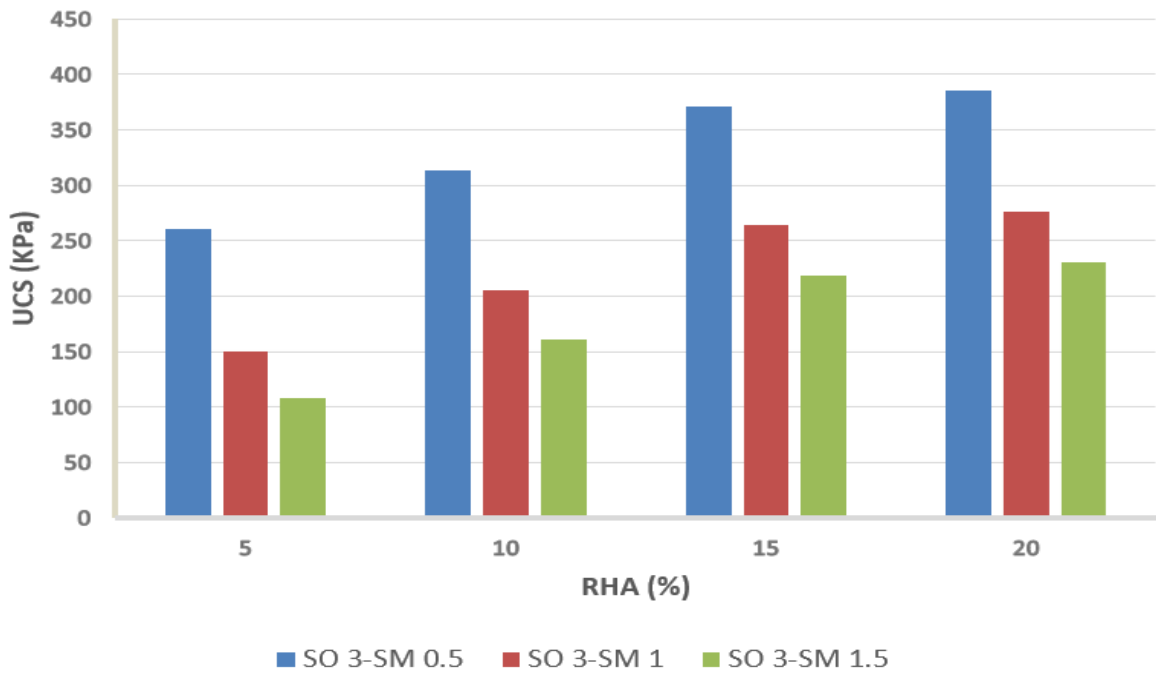


Figure 4.11- UCS Results of Set 2 (7 days cured)

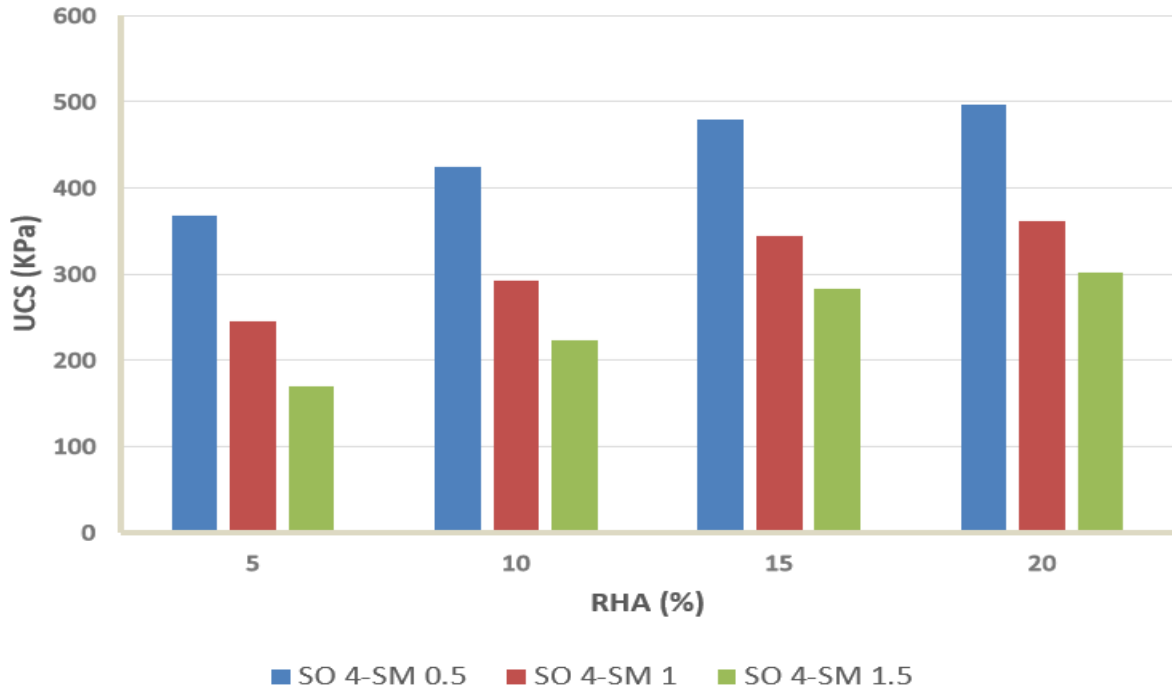


Figure 4.12- UCS Results of Set 3 (7 days cured)

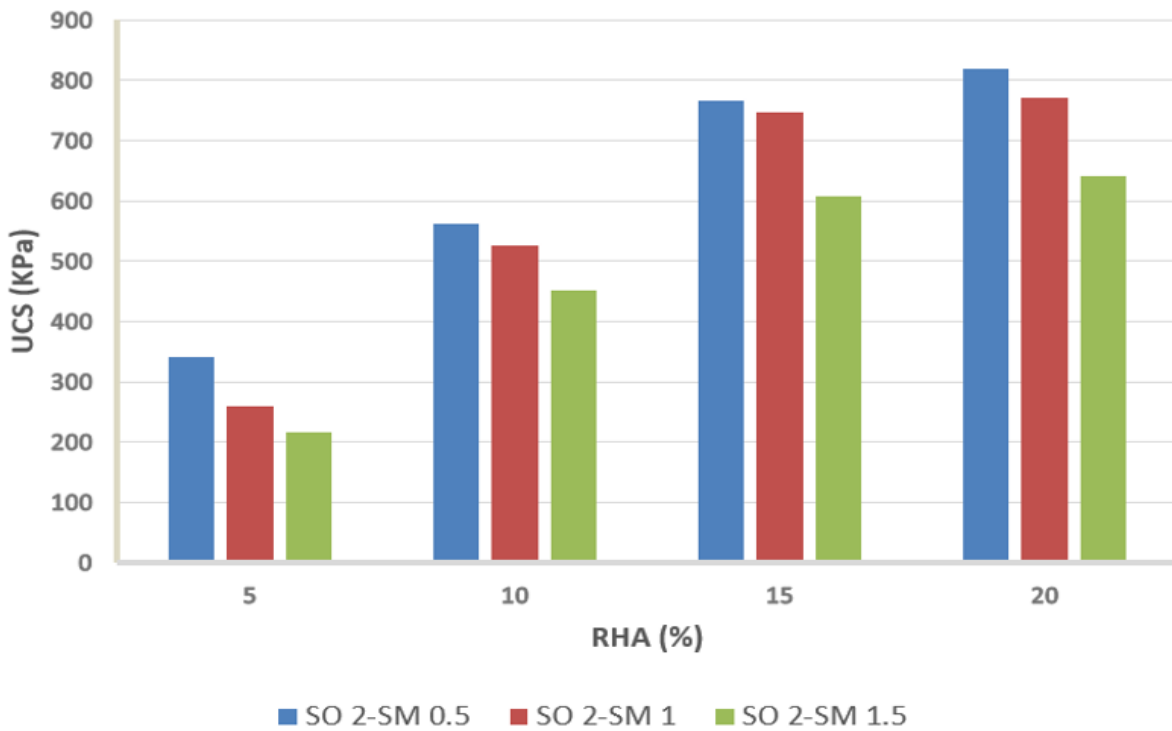


Figure 4.13- UCS Results of Set 1 (28 days cured)

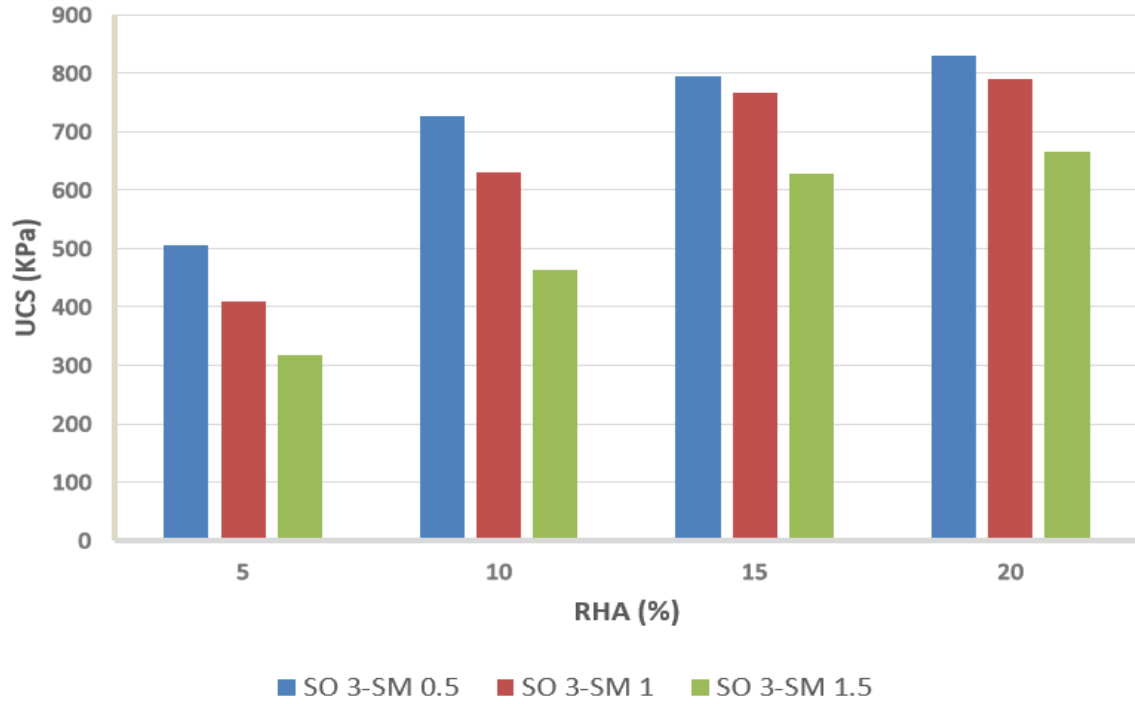


Figure 4.14- UCS Results of Set 2 (28 days cured)

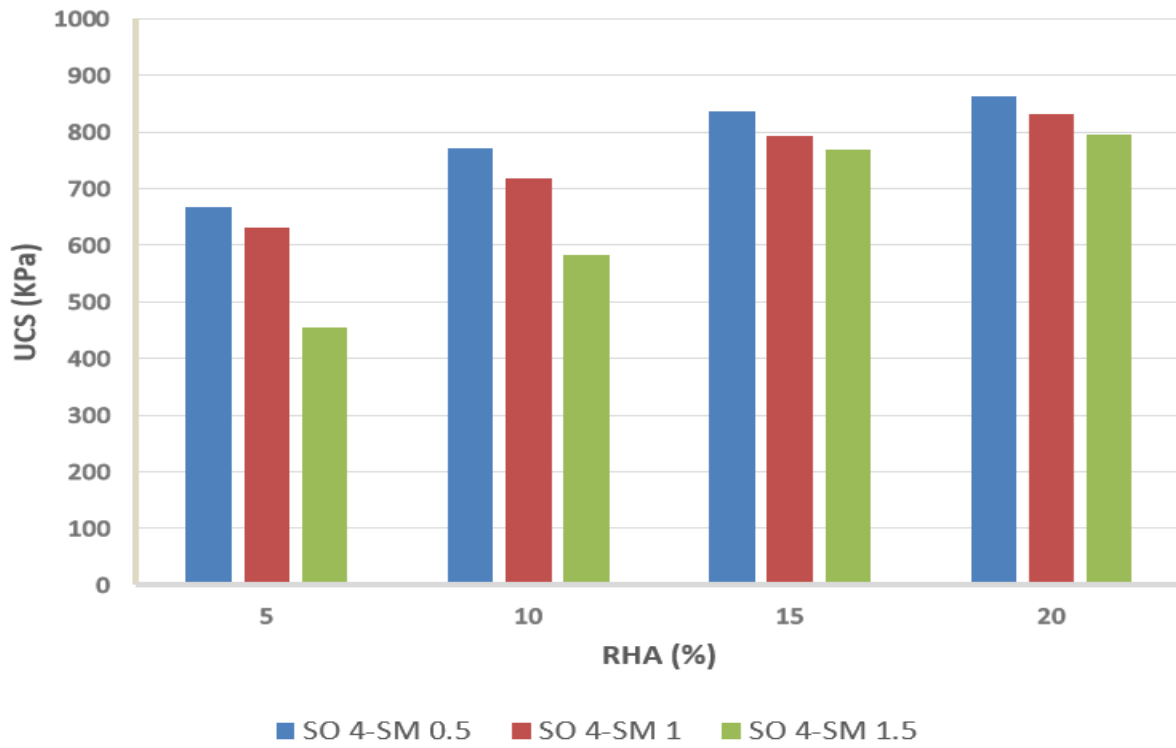


Figure 4.15- UCS Results of Set 3 (28 days cured)

Figure 4.16, Figure 4.17 and Figure 4.18 shows the influence of sodium oxide and silica modulus on the strength improvement. It was found that UCS increased with increase in sodium oxide from 2% to 4%. This is because a higher concentration of sodium oxide results in a stronger alkaline medium and causes a greater amount of RHA to be engaged in the reactions at a given time due to improved dissolving of RHA. Higher quantities of RHA are dissolved, leading to more binders (Shukla et al., 2020). With the rise in silica modulus, the compressive strength decreased, and the variation is shown in Figures 4.19, 4.20 and 4.21. Excess SiO₂ precipitates, creating adverse effects such as efflorescence, pH reduction and increased binder viscosity (Adewumi et al., 2020). Figure 4.22 shows the formation of efflorescence. The compressive strength of all specimens rose as the number of curing days increased.

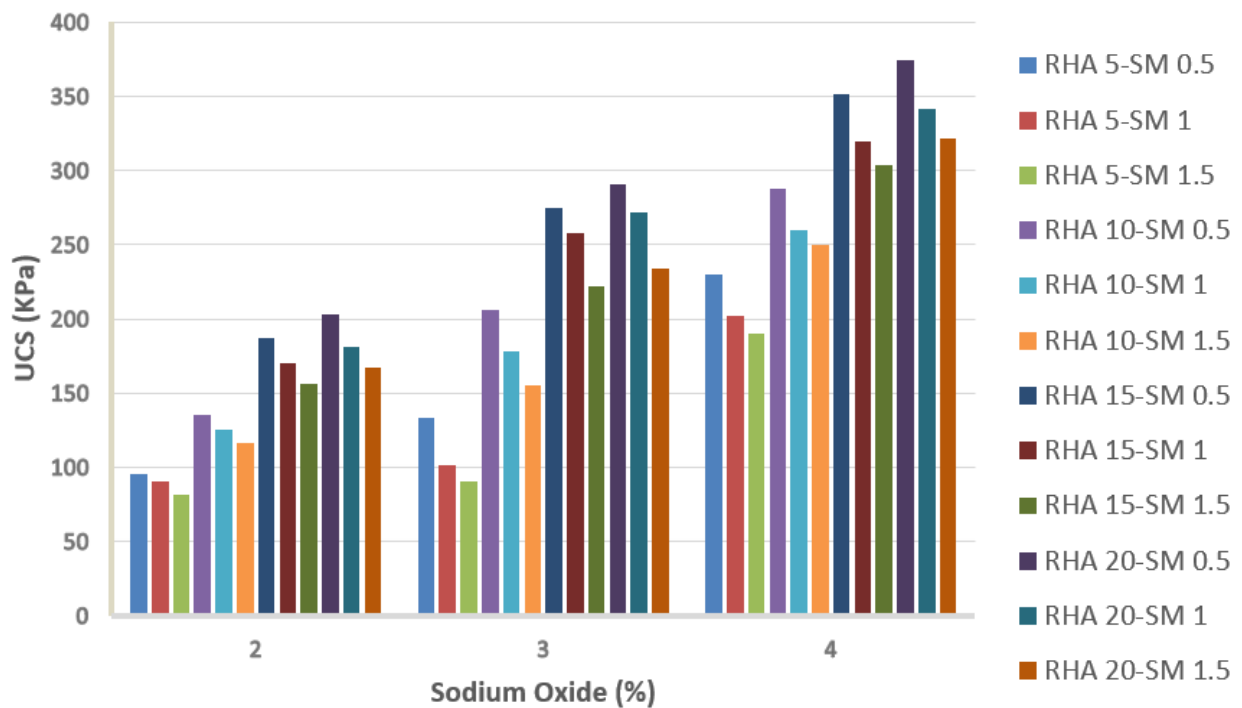


Figure 4.16- Variation in UCS with Increase in Sodium Oxide (3 days cured)

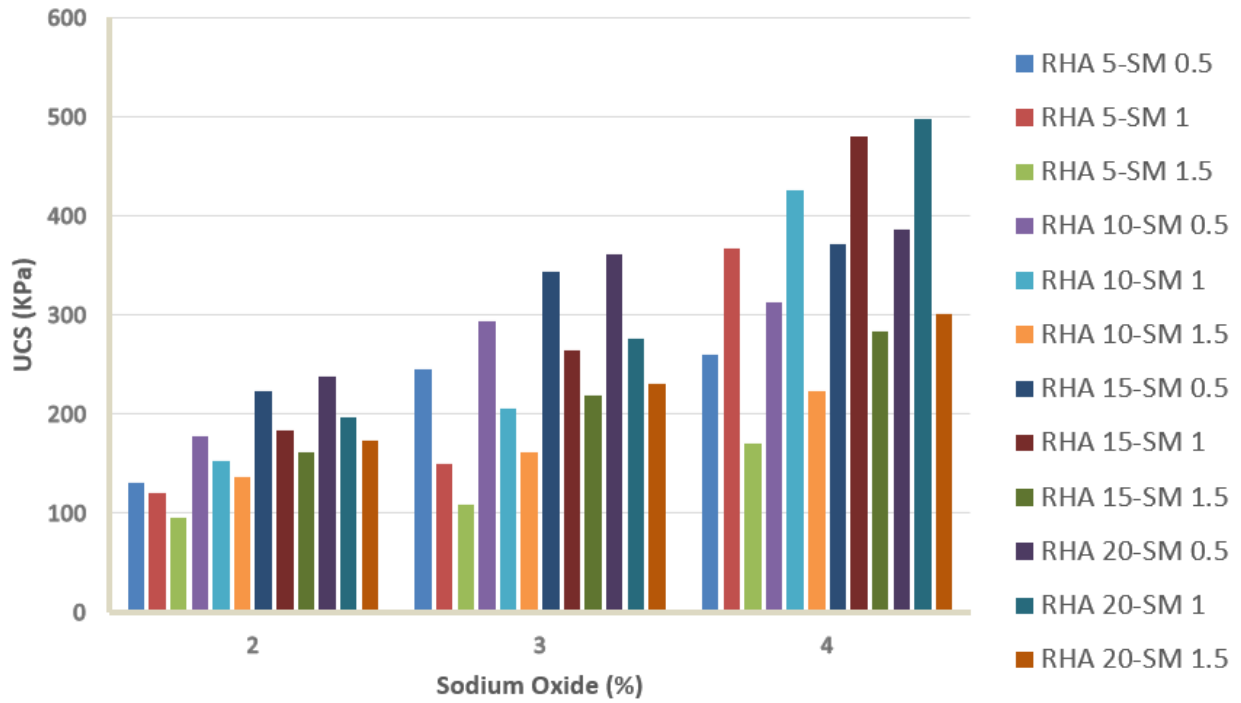


Figure 4.17- Variation in UCS with Increase in Sodium Oxide (7 days cured)

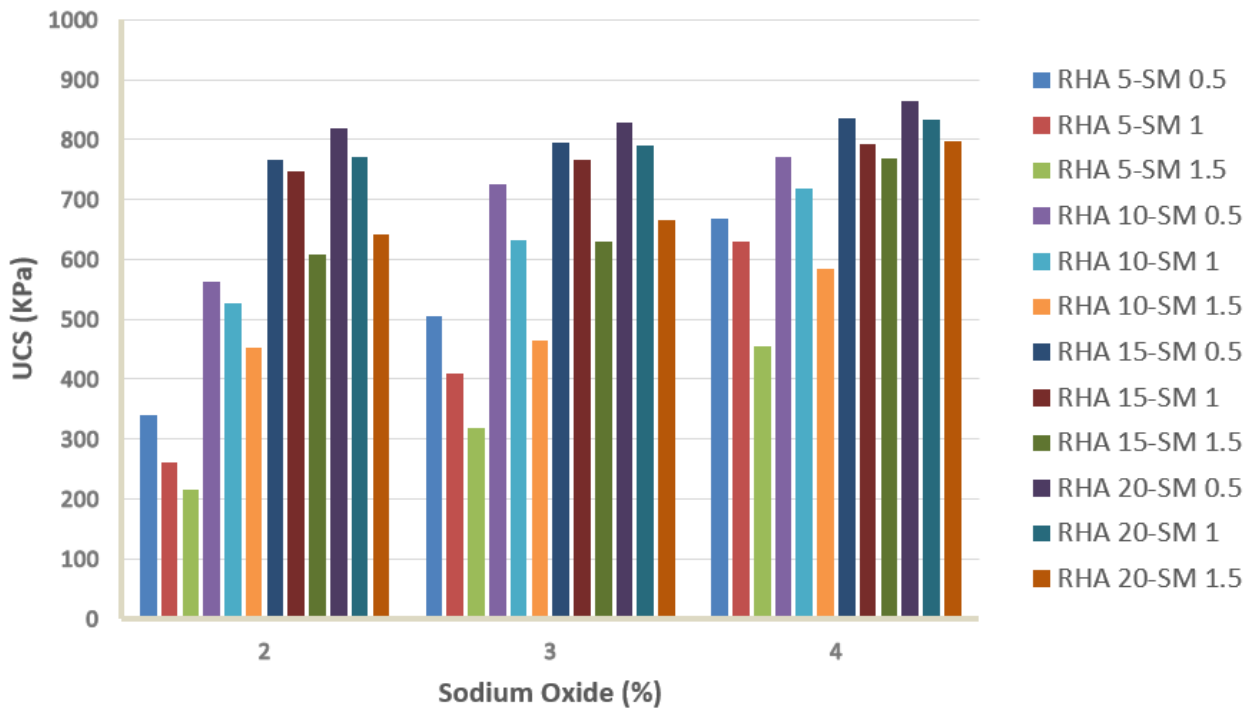


Figure 4.18- Variation in UCS with Increase in Sodium Oxide (28 days cured)

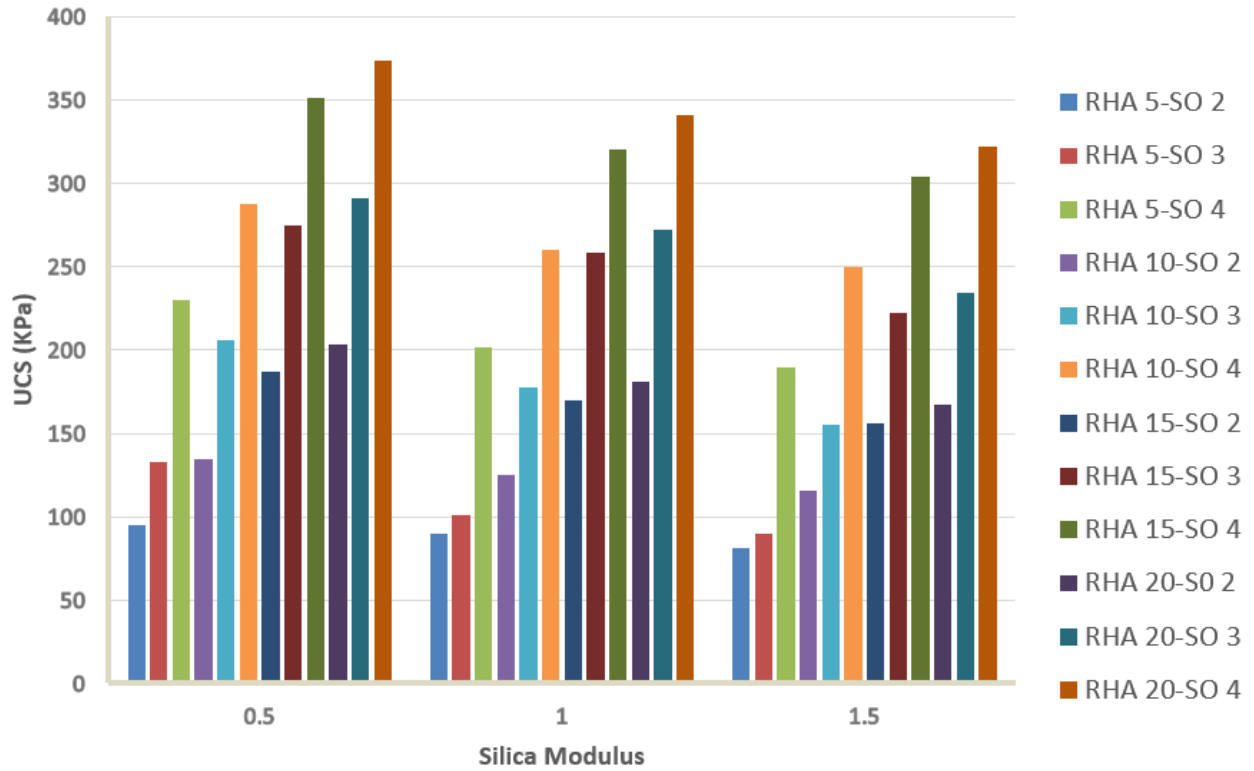


Figure 4.19- Variation in UCS with Increase in Silica Modulus (3 days cured)

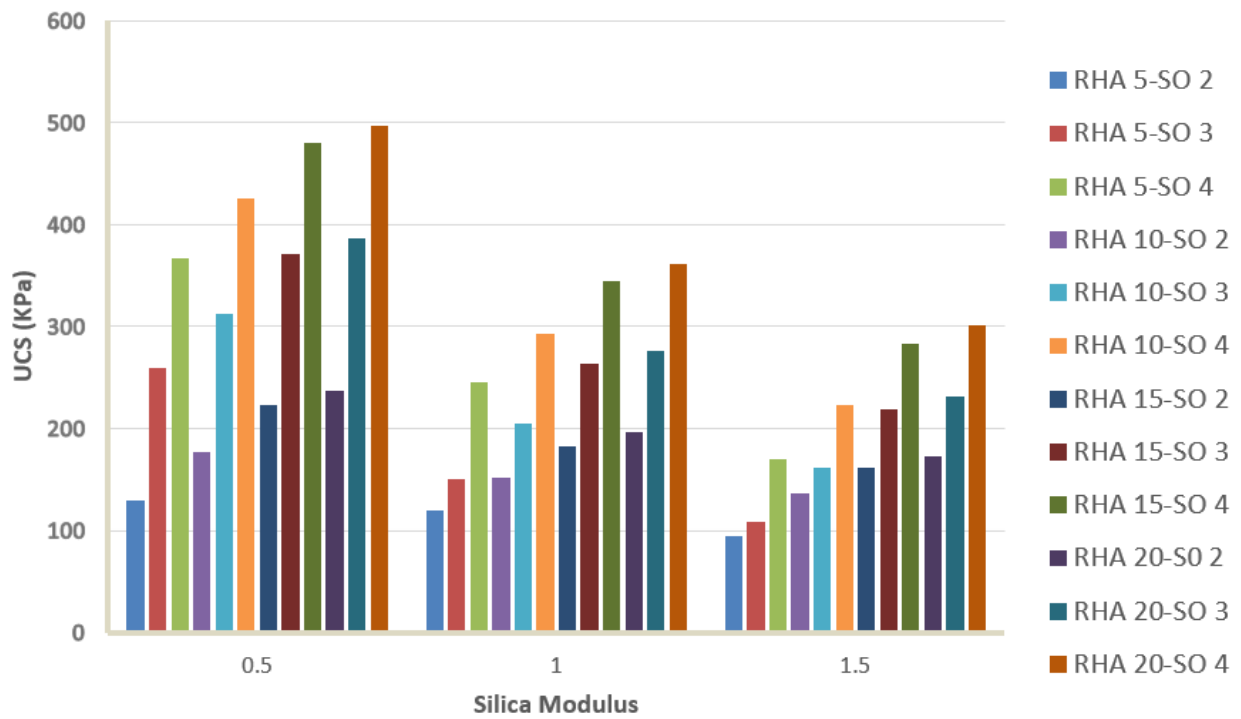


Figure 4.20- Variation in UCS with Increase in Silica Modulus (7 days cured)

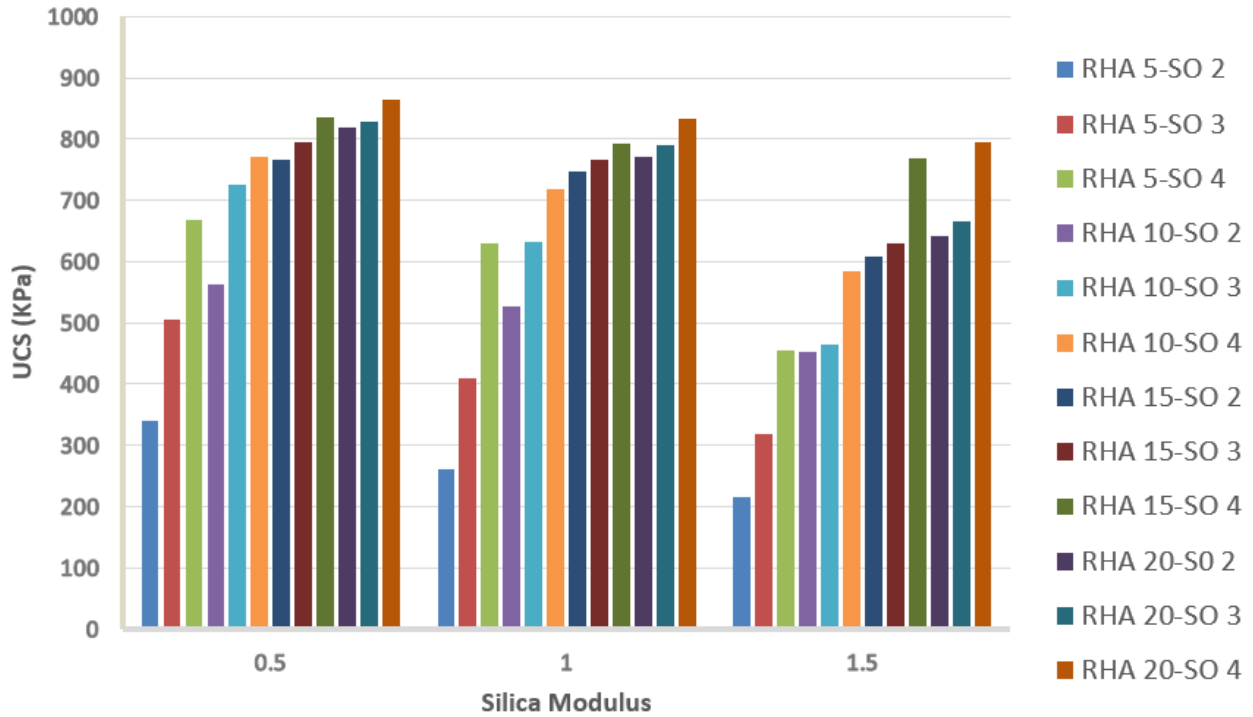


Figure 4.21- Variation in UCS with Increase in Silica Modulus (28 days cured)



Figure 4.22- Formation of Efflorescence

4.3.2 Durability Test

WD test was done on 3, 7 and 28 days cured samples of all 36 combinations. All the samples failed the test after 3 and 7 days of curing. Thirty three sample combinations failed the test after 28 days of curing. After curing for 28 days, only the samples RHA 10-SO 4-SM 0.5, RHA 15-SO 4-SM 0.5 and RHA 20-SO 4-SM 0.5 passed the Durability Test after 12 cycles with weight loss below

14%. Sample RHA 20-SO 4-SM 0.5 has the least weight loss. The Durability Test result is shown in Figure 4.23.

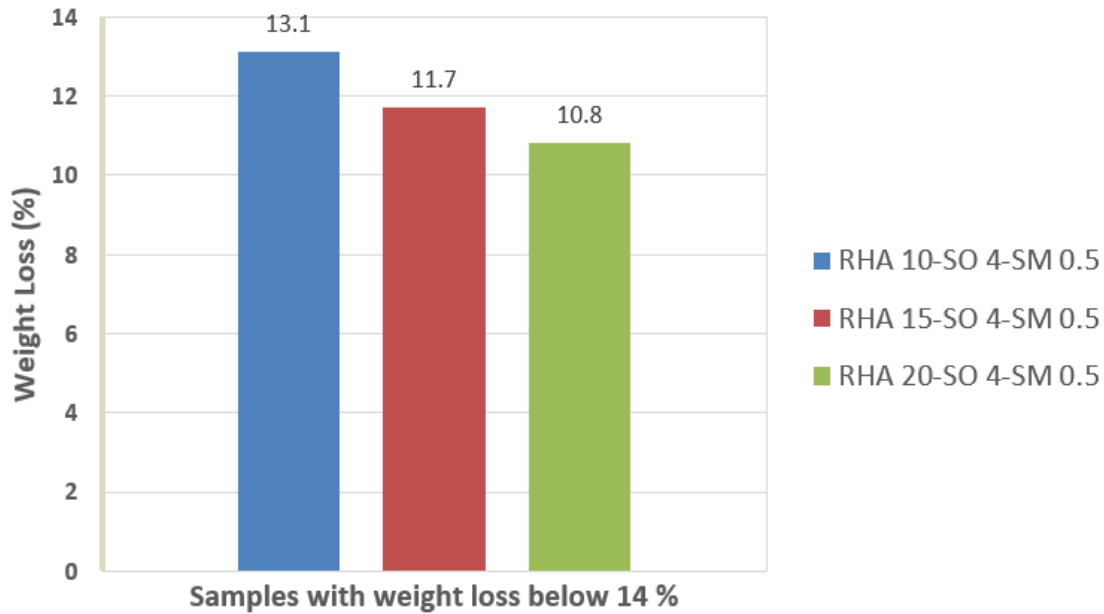


Figure 4.23- Durability Test Results

RHA 10-SO 4-SM 0.5, RHA 15-SO 4-SM 0.5, and RHA 20-SO 4-SM 0.5 are the samples with maximum UCS values and only these samples have passed the Durability Test after curing for 28 days. So further tests were done only on these samples with better performance.

4.3.3 CBR test

CBR Test was done on samples RHA 10-SO 4-SM 0.5, RHA 15-SO 4-SM 0.5 and RHA 20-SO 4-SM 0.5. The CBR value of raw BCS was 2.3. The CBR values also increased with the rise in RHA from 10% to 20% and with a rise in curing time. Soaked and unsoaked CBR values of 3,7 and 28 days cured specimens are shown in Figures 4.24 and 4.25, respectively. Sample RHA 20-SO 4-SM 0.5 has the highest CBR value in both soaked and unsoaked conditions.

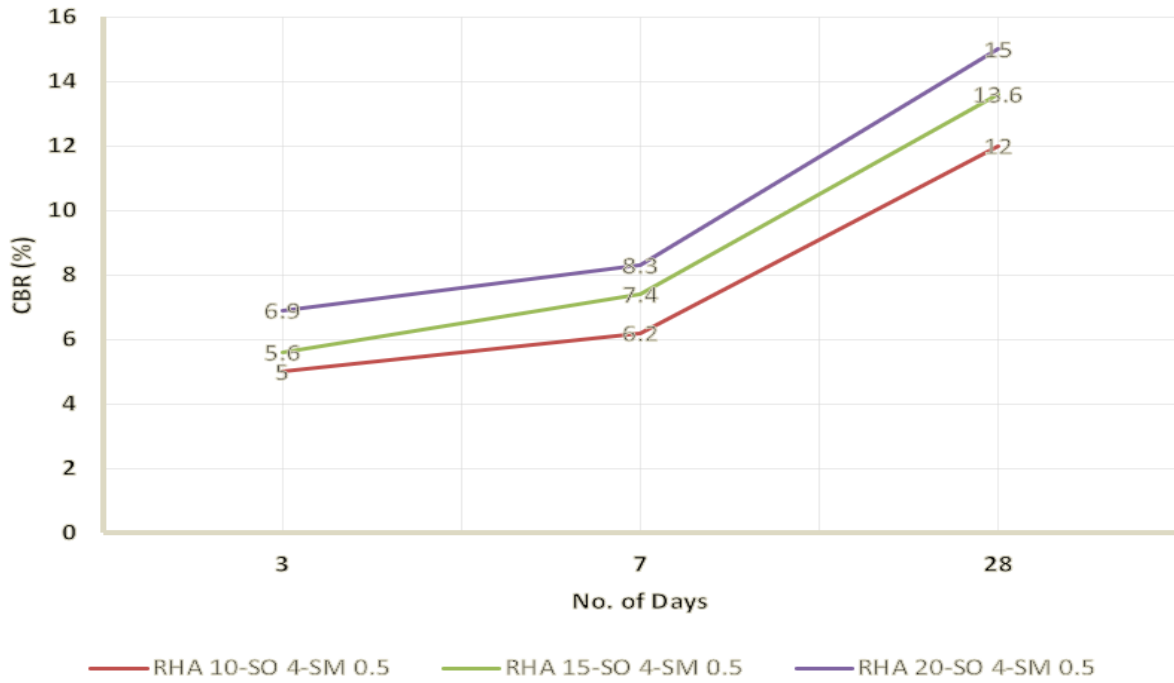


Figure 4.24- Soaked CBR Results

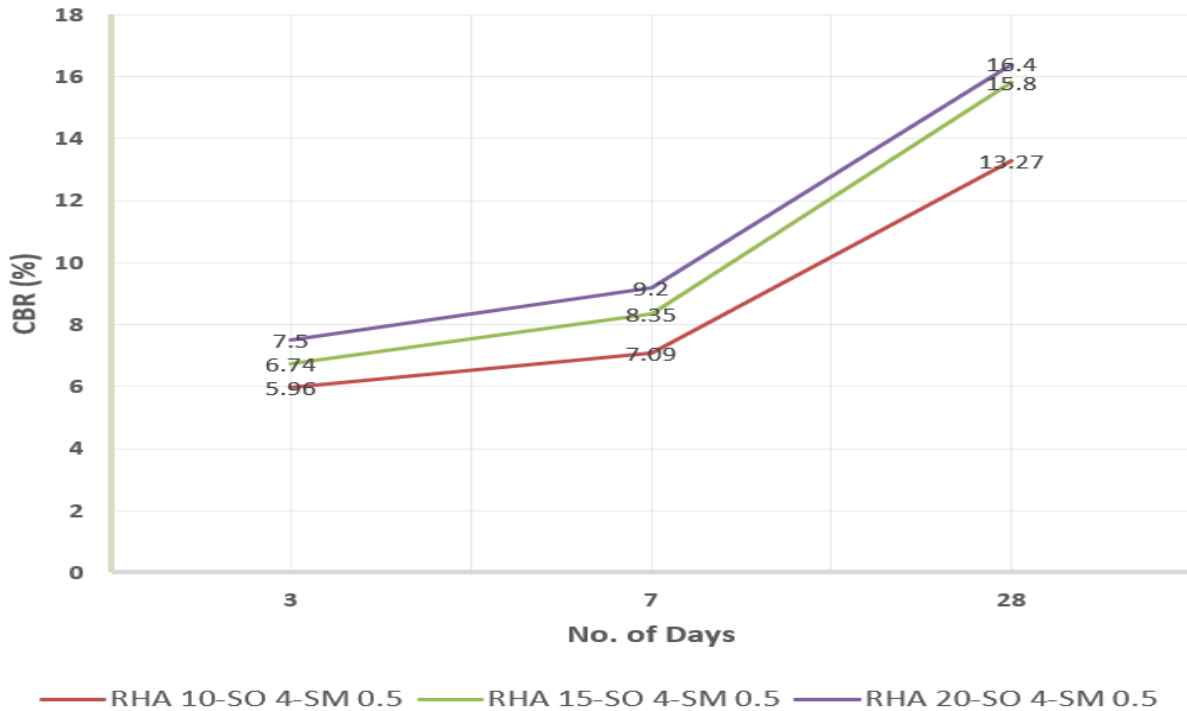


Figure 4.25- Unsoaked CBR Results

4.3.4 Swelling Test

This test was done on specimens RHA 10-SO 4-SM 0.5, RHA 15-SO 4-SM 0.5 and RHA 20-SO 4-SM 0.5. The free swell index of raw BCS was 38.2%. With increased RHA content from 10% to 20% and a rise in curing time, the free swell index was also reduced. Due to improved soil binding lesser surface area of soil particles was exposed to water and underwent less swelling (Murmu et al., 2019). Free swell index of 3, 7 and 28 days cured specimens are shown in Figure 4.26. Sample RHA 20-SO 4-SM 0.5 has the lowest free swell index value.

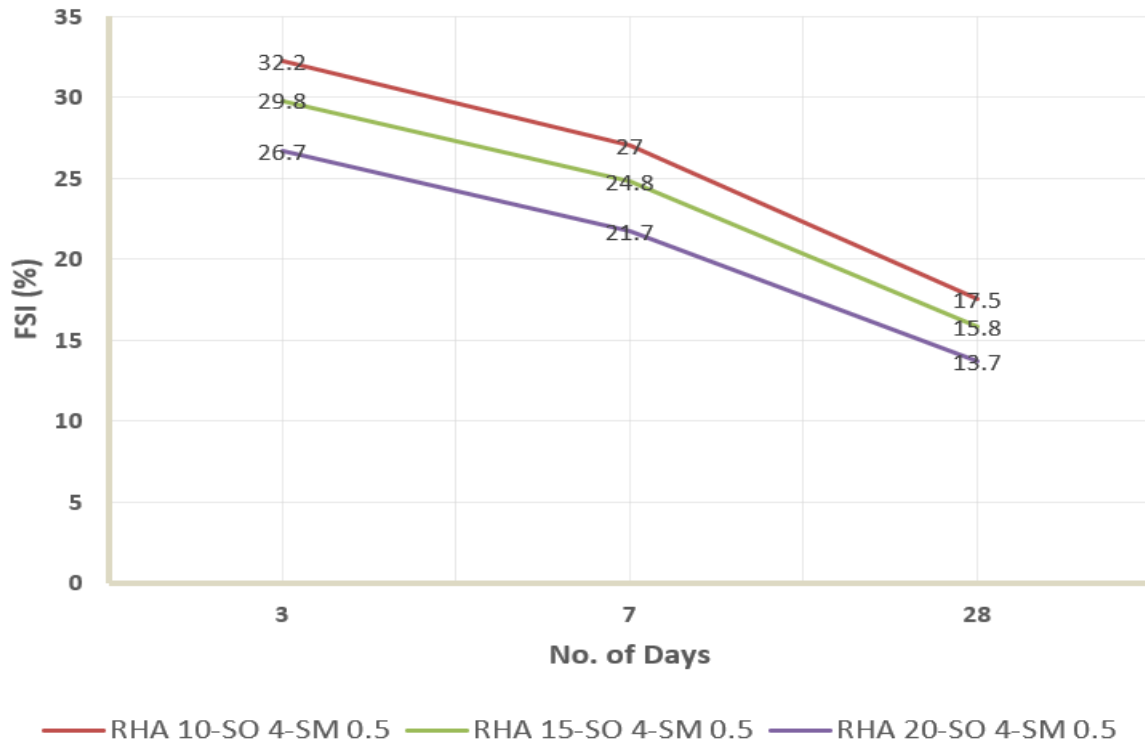


Figure 4.26- Free Swell Index Values

4.3.5 Flexural Strength Test

This test has been done on specimens RHA 10-SO 4-SM 0.5, RHA 15-SO 4-SM 0.5 and RHA 20-SO 4-SM 0.5 after 3, 7 and 28 days of curing. The flexural strength of these samples is shown in Figure 4.27. The flexural strength of raw BCS was 0.13 MPa. Sample RHA 20-SO 4-SM 0.5 has the highest flexural strength.

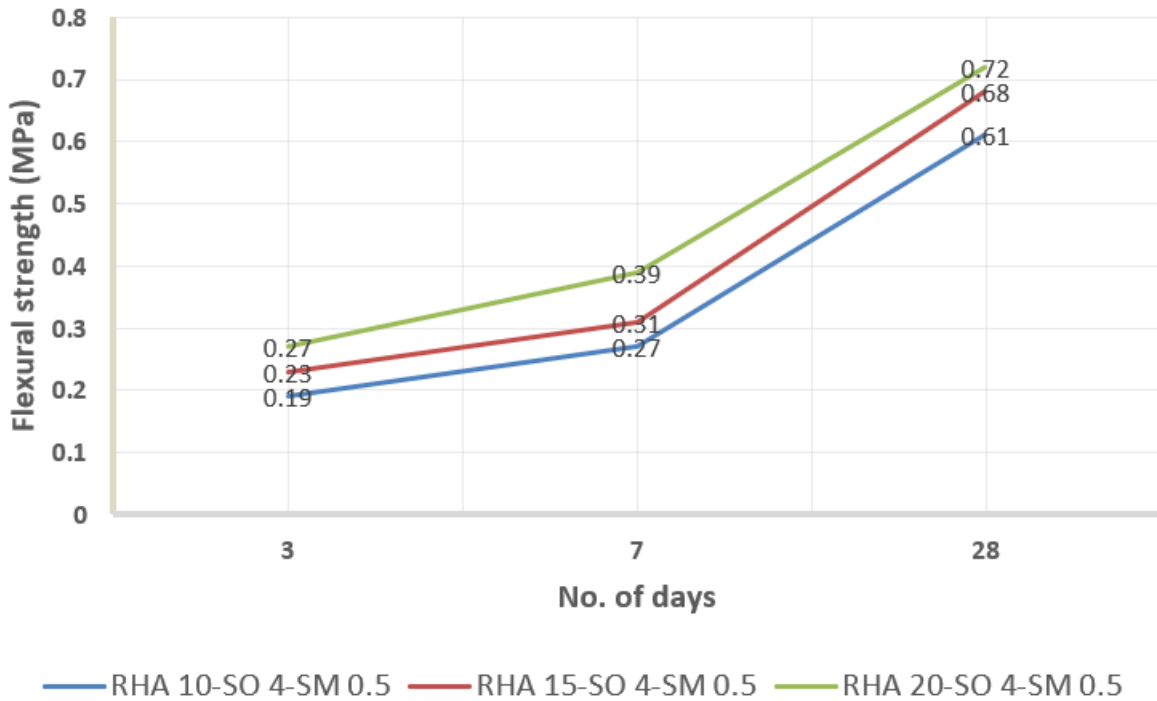


Figure 4.27- Flexural Strength Test Results

4.4 Pavement Design

Pavement design was done on IITPAVE based on IRC 37-2018. Designing was based on the soaked CBR value of the sample RHA 20-SO 4-SM 0.5 after 28 days of curing. The design was done with 90% reliability at a set cumulative traffic load of 18 msa (From Equation 4.5 of IRC 37-2018). The highest soaked CBR value was 15% for the sample RHA 20-SO 4-SM 0.5. The design was proposed for the Kozhinjampara-Nadupuni road stretch located in Palakkad. Effective CBR was found to be 7%. A trial section was selected from plate 3 of IRC 37- 2018 and the thickness of each layer is

- Surface course- 30 mm
- Base/Binder Course- 95 mm
- Wet Mix Macadam- 250 mm
- Granular Subbase- 200 mm

Figure 4.28 shows the input data of IITPAVE and Figure 4.29 shows the critical strain locations.

No of Layers HOME

Layer: 1	Elastic Modulus(MPa)	<input type="text" value="3000"/>	Poisson's Ratio	<input type="text" value="0.35"/>	Thickness(mm)	<input type="text" value="30"/>
Layer: 2	Elastic Modulus(MPa)	<input type="text" value="3000"/>	Poisson's Ratio	<input type="text" value="0.35"/>	Thickness(mm)	<input type="text" value="100"/>
Layer: 3	Elastic Modulus(MPa)	<input type="text" value="128"/>	Poisson's Ratio	<input type="text" value="0.35"/>	Thickness(mm)	<input type="text" value="450"/>
Layer: 4	Elastic Modulus(MPa)	<input type="text" value="59"/>	Poisson's Ratio	<input type="text" value="0.35"/>		

Wheel Load(Newton) Tyre Pressure(MPa)

Analysis Points

Point:1	Depth(mm):	<input type="text" value="130"/>	Radial Distance(mm):	<input type="text" value="0"/>
Point:2	Depth(mm):	<input type="text" value="130"/>	Radial Distance(mm):	<input type="text" value="155"/>
Point:3	Depth(mm):	<input type="text" value="580"/>	Radial Distance(mm):	<input type="text" value="0"/>
Point:4	Depth(mm):	<input type="text" value="580"/>	Radial Distance(mm):	<input type="text" value="155"/>

Wheel Set (1- Single wheel
2- Dual wheel)

Figure 4.28- Input Data of IITPAVE

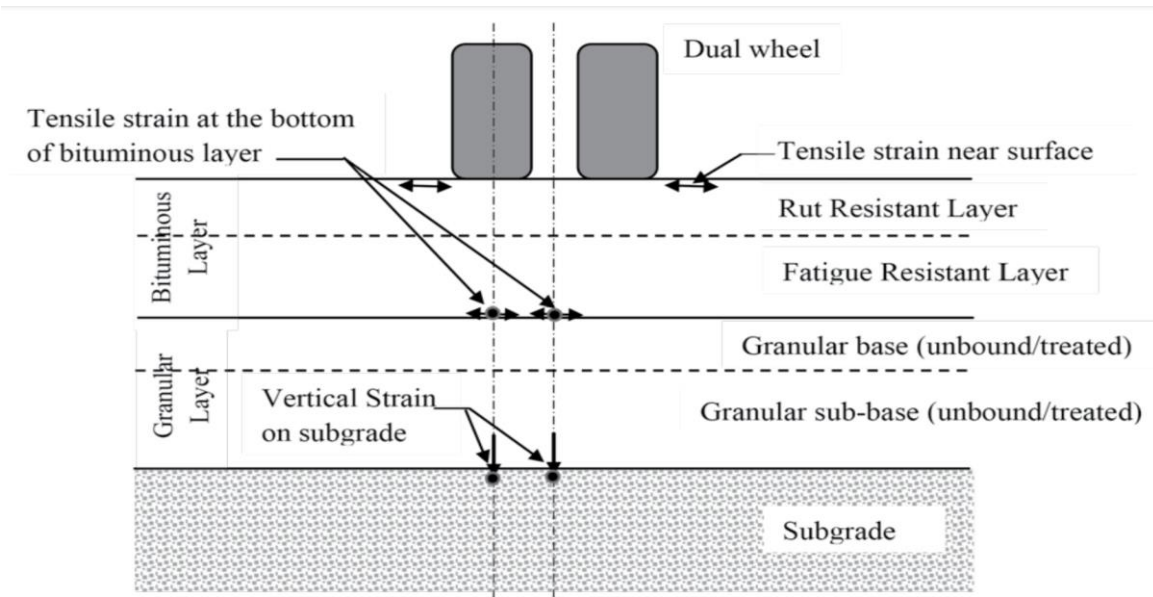


Figure 4.29- Locations of Critical Strain

(Source: IRC 37- 2018)

4.5 Closure

The stabilized soil samples were subjected to different laboratory tests. CBR value, UCS value and flexural strength were improved and three stabilized samples passed the durability test. The method was also efficient in lowering the free swell index of soil. The pavement was designed based on the soaked CBR value of the sample RHA 20-SO 4-SM 0.5 and the design was safe.

CHAPTER 5

SUMMARY AND CONCLUSION

5.1 Summary

The application of alkali activated RHA to stabilize BCS has been discussed in this work. The alkalis used for activation include sodium hydroxide and sodium silicate. Sodium oxide (Na_2O) and silica modulus (Ms) were the activator parameters selected for the investigation and were varied in different proportions. Unconfined Compression Strength Test and Durability Test were used to study the effect of different proportions of alkali activated RHA and activator parameters at different curing durations. The CBR, Swelling and Flexural Strength Test were done on samples that passed the Durability Test and with the highest compressive strength. This soil treatment enhanced the CBR, Unconfined Compressive Strength (UCS), durability and flexural strength of the BCS and reduced swelling. The pavement was designed based on the maximum soaked CBR value using IITPAVE software. BCS improved engineering properties when treated with alkali activated RHA. The major conclusions of this study are listed in this chapter.

5.2 Conclusions

- With the increase in sodium oxide, the strength has been observed to increase and with an increase in silica modulus, the strength was found to decrease
- Sample RHA 20-SO 4-SM 0.5 has better performance in all the tests
- UCS was improved with an increase in RHA content. Maximum UCS of 864 KPa for the sample RHA 20-SO 4-SM 0.5 - 8 times increase in UCS after 28 days of curing
- Minimum weight loss of 10.8% in durability test for the sample RHA 20-SO 4-SM 0.5 after 28 days of curing
- Maximum unsoaked CBR of 16.2% for the sample RHA 20-SO 4-SM 0.5 - 5 times increase in unsoaked CBR after 28 days of curing
- Maximum soaked CBR of 15% for the sample RHA 20-SO 4-SM 0.5 - 6 times increase in soaked CBR after 28 days of curing

- Free swell index was reduced from 38.2% to 13.7% for the sample RHA 20-SO 4-SM 0.5 and soil has a low degree of expansiveness
- Maximum flexural strength of 0.72 MPa for the sample RHA 20-SO 4-SM 0.5 - 5 times increase in flexural strength
- Critical strain analysis was carried out using IITPAVE and found that strains are within the limits and therefore, the design is safe
- Alkali activated RHA can be used as an eco-friendly binder instead of Portland Cement to improve the engineering properties of subgrade soil

5.3 Research Contributions

Most research on the alkali activation method has employed fly ash or slag as precursors. Much research has been conducted that shows the efficacy of fly ash and slag in alkali activation. There have been limited studies on the effectiveness of other precursors such as RHA, palm oil fuel ash, red mud, paper sludge ash etc. Most studies include these materials as secondary materials together with fly ash or slag. A less explored precursor like RHA for soil stabilization using alkali activation was introduced and how the variation of essential parameters like sodium oxide and silica modulus can affect the strength of the soil in alkali activation was studied.

5.4 Limitations and Future Scope

- Due to time limitations, only the improvement in UCS, CBR, durability, swelling and flexural strength was studied
- Other tests can also be done to study the permeability, variation in shear strength parameters, fatigue strength, compressibility etc
- Microstructural analysis like SEM can be done
- Other alkalis like lithium and magnesia can be used and many other precursors like meta kaoline, red mud, coffee husk ash etc, can also be used
- This method can be done on different soil types and results can be compared

REFERENCES

1. Abdeldjouad, L., Asadi, A., Nahazanan, H., Huat, B. B., Dheyab, W., & Elkhebu, A. G. (2019). Effect of clay content on soil stabilization with alkaline activation. *International Journal of Geosynthetics and Ground Engineering*, 5(1), 1-8.
2. Abhilash, H. N., Walker, P., Venkatarama Reddy, B. V., Heath, A., & Maskell, D. (2020). Compressive strength of novel alkali-activated stabilized earth materials incorporating solid wastes. *Journal of Materials in Civil Engineering*, 32(6), 04020118.
3. Adewumi, A. A., Mohd Ariffin, M. A., Maslehuddin, M., Yusuf, M. O., Ismail, M., & Al-Sodani, K. A. A. (2021). Influence of silica modulus and curing temperature on the strength of alkali-activated volcanic ash and limestone powder mortar. *Materials*, 14(18), 5204
4. Amulya, S., & Ravi Shankar, A. U. (2020). Replacement of conventional base course with stabilized lateritic soil using ground granulated blast furnace slag and alkali solution in the flexible pavement construction. *Indian Geotechnical Journal*, 50, 276-288.
5. Amulya, S., Ravi Shankar, A. U., & Praveen, M. (2020). Stabilization of lithomargic clay using alkali activated fly ash and ground granulated blast furnace slag. *International Journal of Pavement Engineering*, 21(9), 1114-1121.
6. Mohan, K., & Kumar, P. (2020). Analysis of Flexible Pavement using IITPAVE Software and Economic Analysis of the Project using HDM-4 Software. *International Journal for Research in Applied Science & Engineering Technology*, 8.
7. Bahmani, M., Fatehi, H., Noorzad, A., & Hamedi, J. (2019). Biological soil improvement using new environmental bacteria isolated from northern Iran. *Environmental Geotechnics*, 40, 1-13.
8. Chen, R., Zhu, Y., & Bao, W. (2020). Stabilization of soft soil using low-carbon alkali-activated binder. *Environmental Earth Sciences*, 79(22), 1-13.
9. Cristelo, N., Glendinning, S., Miranda, T., Oliveira, D., & Silva, R. (2012). Soil stabilization using alkaline activation of fly ash for self-compacting rammed earth construction. *Construction and building materials*, 36, 727-735.
10. Cristelo, N., Soares, E., Rosa, I., Miranda, T., Oliveira, D. V., Silva, R. A., & Chaves, A. (2013). Rheological properties of alkaline activated fly ash used in jet grouting applications. *Construction and Building Materials*, 48, 925-933.

11. Du, Y. J., Bo, Y. L., Jin, F., & Liu, C. Y. (2016). Durability of reactive magnesia-activated slag-stabilized low plasticity clay subjected to drying–wetting cycle. *European Journal of Environmental and Civil Engineering*, 20(2), 215-230.
12. Duxson, P. S. W. M., Mallicoat, S. W., Lukey, G. C., Kriven, W. M., & Van Deventer, J. S. (2007). The effect of alkali and Si/Al ratio on the development of mechanical properties of metakaolin-based geopolymers. *Colloids and Surfaces A: Physicochemical and Engineering Aspects*, 292(1), 8-20.
13. Environment, U. N., Scrivener, K. L., John, V. M., & Garter, E. M. (2018). Eco-efficient cements: potential economically viable solutions for a low CO₂ Cement based material industry. *Cement and Concrete Research*, 114, 2-26
14. Ghadir, P., Zamanian, M., Mahbubi-Motlagh, N., Saberian, M., Li, J., & Ranjbar, N. (2021). Shear strength and life cycle assessment of volcanic ash-based geopolymer and cement stabilized soil: A comparative study. *Transportation Geotechnics*, 31, 100639.
15. Harish, G. R., (2017). Analysis of Flexible Pavement Design Using IITPAVE. *Imperial Journal of Interdisciplinary Research (IJIR)*, 3(6), 815-818.
16. Jahandari, S., Tao, Z., Saberian, M., Shariati, M., Li, J., Abolhasani, M., & Rashidi, M. (2021). Geotechnical properties of lime-geogrid improved clayey subgrade under various moisture conditions. *Road Materials and Pavement Design*, 1-19.
17. Lahoti, M., Tan, K. H., & Yang, E. H. (2019). A critical review of geopolymer properties for structural fire-resistance applications. *Construction and Building Materials*, 221, 514-526.
18. Lang, L., Chen, B., & Chen, B. (2021). Strength evolutions of varying water content-dredged sludge stabilized with alkali-activated ground granulated blast-furnace slag: *Construction and Building Materials*, 275, 122111.
19. Lemougna, P. N., Wang, K. T., Tang, Q., Nzeukou, A. N., Billong, N., Melo, U.C. & Cui, X.M. (2018). Review on the use of volcanic ashes for engineering applications. *Resources, Conservation and Recycling*, 137, 177-190.
20. Marvila, M. T., Azevedo, A. R. G. D., & Vieira, C. M. F. (2021). Reaction mechanisms of alkali-activated materials. *IBRACON Structures and Materials Journal*, 14.

21. Mavroulidou, M., Gray, C., Gunn, M. J., & Pantoja-Muñoz, L. (2021). A study of innovative alkali-activated binders for soil stabilization in the context of engineering sustainability and circular economy. *Circular Economy and Sustainability*, 1-25.
22. Mazhar, S., & GuhaRay, A. (2021). Stabilization of expansive clay by fiber-reinforced alkali-activated binder: an experimental investigation and prediction modelling. *International Journal of Geotechnical Engineering*, 15(8), 977-993.
23. McLellan, B. C., Williams, R. P., Lay, J., Van Riessen, A., & Corder, G. D. (2011). Costs and carbon emissions for geopolymer pastes in comparison to ordinary Portland cement. *Journal of cleaner production*, 19(9-10), 1080-1090.
24. Miraki, H., Shariatmadari, N., Ghadir, P., Jahandari, S., Tao, Z., & Siddique, R. (2022). Clayey soil stabilization using alkali-activated volcanic ash and slag. *Journal of Rock Mechanics and Geotechnical Engineering*, 14(2), 576-591.
25. Murmu, A. L., Jain, A., & Patel, A. (2019). Mechanical properties of alkali activated fly ash geopolymer stabilized expansive clay. *KSCE Journal of Civil Engineering*, 23(9), 3875-3888.
26. Murmu, A. L., Jain, A., & Patel, A. (2019). Mechanical properties of alkali activated fly ash geopolymer stabilized expansive clay. *KSCE Journal of Civil Engineering*, 23(9), 3875-3888.
27. Phetchuay, C., Horpibulsuk, S., Arulrajah, A., Suksiripattanapong, C., & Udomchai, A. (2016). Strength development in soft marine clay stabilized by fly ash and calcium carbide residue based geopolymer. *Applied clay science*, 127, 134-142.
28. Provis, J. L., & Bernal, S. A. (2014). Geopolymers and related alkali-activated materials. *Annual Review of Materials Research*, 44, 299-327.
29. Saberian, M., Li, J., Perera, S. T. A. M., Ren, G., Roychand, R., & Tokhi, H. (2020). An experimental study on the shear behaviour of recycled concrete aggregate incorporating recycled tyre waste. *Construction and Building Materials*, 264, 120266.
30. Sadeghian, F., Jahandari, S., Haddad, A., Rasekh, H., & Li, J. (2022). Effects of variations of voltage and pH value on the shear strength of soil and durability of different electrodes and piles during electrokinetic phenomenon. *Journal of Rock Mechanics and Geotechnical Engineering*, 14(2), 625-636.

31. Sargent, P., Hughes, P. N., Rouainia, M., & White, M. L. (2013). The use of alkali activated waste binders in enhancing the mechanical properties and durability of soft alluvial soils. *Engineering geology*, 152(1), 96-108.
32. Shukla, A., Chaurasia, A. K., Mumtaz, Y., & Pandey, G. (2020). Effect of Sodium Oxide on Physical and Mechanical properties of Fly-Ash based geopolymer composites. *Indian J. Sci. Technol*, 13(38), 3994-4002.
33. Tan, T., Huat, B. B., Anggraini, V., Shukla, S. K., & Nahazanan, H. (2021). Strength behavior of fly ash-stabilized soil reinforced with coir fibers in alkaline environment. *Journal of Natural Fibers*, 18(11), 1556-1569.
34. Thomas, A., Tripathi, R. K., & Yadu, L. K. (2018). A laboratory investigation of soil stabilization using enzyme and alkali-activated ground granulated blast-furnace slag. *Arabian Journal for Science and Engineering*, 43(10), 5193-5202.
35. Turner, L.K., & Collins, F.G. (2013). Carbon dioxide equivalent (CO₂-e) emissions: A comparison between geopolymer and OPC cement concrete. *Construction and building materials*, 43, 125-130.
36. Visvanathan, A., Velayudhan, S., & Mathew, S. (2022). Field evaluation of coir geotextile reinforced subgrade for low volume pavements. *Journal of Natural Fibers*, 19(2), 597-609.
37. Wu, Y., Lu, B., Bai, T., Wang, H., Du, F., Zhang, Y., & Wang, W. (2019). Geopolymer, green alkali activated cementitious material: Synthesis, applications and challenges. *Construction and Building Materials*, 224, 930-949.

APPENDIX

Sample Calculation

Calculation of sample RHA 20-SO 4- SM 1 (Done for 1kg of BCS)

- Quantity of RHA = $(20/100) \times 1000$ grams = 200 grams
- Quantity of BCS = 1000 grams - 200 grams = 800 grams
- Quantity of Sodium Oxide = $(4/100) \times 200$ = 8g
- Silica oxide/sodium oxide = 1
Quantity of Silica Oxide = 1 x sodium oxide = 1 x 8 grams = 8 grams
- 1000 grams of sodium silicate has 325 grams of silica oxide
To get 8 grams of silica oxide, $8 \times 1000 / 325 = 24.61$ grams of sodium silicate is needed
- 1000 grams of sodium silicate has 18.7 grams of sodium oxide
24.61 grams of sodium silicate has $24.61 \times 18.7 / 1000 = 4.6$ grams of sodium oxide
- Remaining sodium oxide needed = 8 grams – 4.6 grams = 3.4 grams
- 80 grams of sodium hydroxide has 62 grams of sodium oxide
To get remaining 3.4 grams of sodium oxide, $3.4 \times 80 / 62 = 4.38$ grams of sodium hydroxide is to be added
- 1000 grams of sodium silicate has 488 grams of water
24.61 grams of sodium silicate has $24.61 \times 488 / 1000 = 12$ grams of water
- 80 grams of sodium hydroxide has 18 grams of water
4.38 grams of sodium hydroxide consists of $4.38 \times 18 / 80 = 0.98$ gram of water
- Quantity of water from both the alkali = 12 + 0.98 = 12.98 grams
- Water/binder = 0.25
Water = 200 x 0.25 = 50 grams
- Optimum moisture content = 20 % = $(20/100) \times 800 = 160$ grams
- Water that needs to be added to the mix = 160 – (12.98+50) = 97.02 grams of water